Towards a construction of the realistic model in grand Gauge-Higgs unification

(ゲージ・ヒッグス大統一模型における現実的模型の構築へ向けて)

理学研究科
数物系専攻

令和 4 年度

Yoshiki Yatagai
(矢田貝祥貴)

Abstract

We discuss a $SU(6)$ grand Gauge-Higgs unification (gGHU). In this model, the Standard Model (SM) higgs field is identified with one of the extra spatial components of the higher-dimensional gauge fields. To construct the realistic model we study following three topics.

First, we consider reproducing the Standard Model mass hierarchy. To reproduce it, the SM fermions are introduced on a fixed point in an orbifold compactification and some massive bulk fermions are introduced. SM fermion masses can be generated by integrating out the bulk fermions. However, the top quark mass is not reproduced in this setup. Therefore, we also introduce the localized gauge kinetic terms to enhance the SM masses and we obtain the suitable parameter regions to reproduce the SM fermion mass hierarchy including the top quark mass.

Second, we consider reproducing the flavor mixing angles and a CP phase. To reproduce them, we modify the interactions between the SM and bulk fermions. We can reproduce the flavor mixing angles and a CP phase.

Finally, we consider the gauge coupling unification. Since the gauge coupling runs linearly in the five-dimensional theory, whether the theory is asymptotically free is nontrivial. We show that one of our models is asymptotically free and obtain the GUT scale of 10^{-14} GeV.

This thesis is based on a series of our work [1–4].

Contents

1 Introduction

Standard Model (SM) has been completed by the discovery of the Higgs field as a final peace. The Higgs field plays an important role for understanding the unification of the electromagnetic and weak interactions through the spontaneous symmetry breaking. Unfortunately, the Higgs sector has not been fully understood. Especially, the hierarchy problem is well known, which requires a fine tuning of parameters in the SM to reproduce the Higgs mass 125 GeV. This is due to the discrepancy between the weak scale ($\sim 10^2$ GeV) and the Planck scale ($\sim 10^{19}$ GeV). It may imply the existence of new physics between the weak and the Planck scale.

Gauge-Higgs unification (GHU) [5] is one of the scenarios beyond the Standard Model (BSM) and proposed as a theory solving the hierarchy problem. In GHU, the SM Higgs field is identified with one of the extra spatial components of the higher dimensional gauge fields. As a result, the physical quantities of the Higgs sector can be computed to be finite. regardless of its non-renormalizability. For instance, it is well known that the tree-level Higgs potential cannot be allowed and its quantum corrections are finite due to the higher dimensional gauge symmetry. One-loop and two-loop cases are shown in [6] and [7], respectively.

Grand unified theory (GUT) is the ultimate theory, which unifies the electromagnetic, the weak and the strong interactions. GUT also has the hierarchy problem as the discrepancy between the weak and the GUT scale. Therefore, the extension of GHU to grand unification is a natural direction to explore. As a minimal unified gauge symmetry, an $SU(6)$ grand Gauge-Higgs unification (gGHU) is discussed [8] [1]. In this theory, the SM fermions are embedded into the KK zero-mode of the five-dimensional fermions without the massless exotic fermions. However, the down-type and the charged lepton Yukawa interactions originated from the gauge interaction cannot be allowed since the corresponding left-handed $SU(2)_L$ doublets and right-handed $SU(2)_L$ singlets are embedded into different five-dimensional fermions. This fact seems to be generic in gGHU as long as the SM fermions are embedded into the bulk fermions.

In my doctoral course, I have studied the three topics in $SU(6)$ gGHU with my collaborators; reproducing the fermion mass hierarchy [1, 2]; reproducing the flavor mixing angles [3]; the gauge coupling unification [4]. In this theses, these wil be explained in order.

[1] For earlier attempts and related works, see [9].

In our first study [1, 2], we consider reproducing the SM fermion mass hierarchy in $SU(6)$ gGHU. Since the down-type and charged lepton Yukawa couplings cannot allowed in [8], we have to consider other approaches. Fortunately, a different approach to generate the SM Yukawa couplings in context to GHU has been known [10, 11]. In this approach, the SM fermions are located on the boundaries, which are fixed points in an orbifold compactification, and the massive bulk fermions and its interaction with the SM fermions are also introduced per generation. The SM fermion masses are obtained by integrating out the massive bulk fermions. However, generated masses have the maximum value around weak boson mass, thus the top quark mass, which is roughly twice as much as the weak boson mass, is not reproduced. This fact also seems to be generic in GHU. As a useful approach to solve this problem [10], by introducing the localized gauge kinetic terms on the boundaries, the generated SM fermion masses can be enhanced. In this thesis, we followed this approach. Introducing the localized gauge kinetic terms, the wave function of the gauge fields are modified and become complicated. We computed its solutions in the periodic and anti-periodic field cases, respectively. As a result, we can reproduce the fermion mass hierarchy including the top quark and obtain the suitable parameter regions.

In our second study [3], we consider reproducing the flavor mixing angles and a CP phase in $SU(6)$ gGHU. Unfortunately, they could not be generated in our model [1, 2]. Therefore, we modify the interactions between the SM and bulk fermions to generate the flavor mixing terms. Thanks to the modification, the number of the bulk fermions can be reduced and its interactions with SM fermions become intergenerational. As a result, we can successfully reproduce the fermion mass hierarchy, the flavor mixing angles and a CP phase with good accuracy.

In our third study [4], we discuss the gauge coupling unification in $SU(6)$ gGHU, which should be explored in a context of GHU scenario. It is well known that the gauge coupling runs logarithmically in four-dimensional theory. On the other hand, the gauge coupling runs linearly in flat five-dimensional theory. Therefore, whether the models in [2, 3] are asymptotically free is nontrivial. In fact, the former model [2] cannot be asymptotically free and the latter model [3] is asymptotically free. This is due to reducing the number of the bulk fermion. As a result, the unification scale is found to be 10^{14} GeV.

This thesis is organized as follows. In the next section, we briefly review the $SU(6)$ gGHU. In section 3, the fermion mass hierarchy in $SU(6)$ gGHU is discussed. Introducing

the massive bulk fermions and the localized gauge kinetic terms are explained. In section 4, the flavor mixing angle in $SU(6)$ gGHU is discussed. Is section 5, we study the gauge coupling unification in the two model shown in section 3 and 4. Final section is devoted to our conclusions.

2 Brief Review of gGHU

In this section, we review a grand Gauge-Higgs unification. First, we explain how to reproduce the four-dimensional physical quantities from five dimensional theory. Second, we explain the simplest $SU(6)$ gGHU model.

In this thesis, M and N (μ and ν) are used as the superscript of five(four)-dimensional coordinates, and y denotes the extra dimension.

$$x^M = (x^\mu, x^5), \qquad x^\mu = (x^0, x^1, x^2, x^3), \qquad y \equiv x^5. \tag{2.1}$$

The metric is given by

$$ds^2 = g_{MN} dx^M dx^N, \qquad g_{MN} = \mathrm{diag}(+1, -1, -1, -1, -1). \tag{2.2}$$

When x^μ appears as an argument of the function, we omit the superscript and simply write x,

$$F(x) \equiv F(x^\mu). \tag{2.3}$$

2.1 Higher dimensional theory

Considering the extension of the standard model to the higher dimensional theory, the question arises how the four-dimensional physical quantity is reproduced at the low energy scale. One of the approaches to study is the compactification of extra dimension, where the periodic boundary conditions are imposed on the extra dimension and the invariance under the condition must be satisfied. Especially, when the number of the extra dimension is one, it is called as S^1 compactification:

$$y \cong y + 2\pi R. \tag{2.4}$$

The periodic boundary conditions of the vector field A_M and the fermion are as follows.

$$\begin{aligned} \hat{T}\left[\mathcal{A}_M(x,y)\right] &= T\mathcal{A}_M T^\dagger = \mathcal{A}_M(x, y + 2\pi R), \\ \hat{T}\left[\Psi(x,y)\right] &= T\Psi = \Psi(x, y + 2\pi R), \end{aligned} \tag{2.5}$$

where $\hat{T}$ is the $2\pi R$ translational operator whose eigenvalues are ± 1 and T is the unitary matrix. In S^1 compactification, the fundamental region of the extra dimensional space is the circumference with the radius R.

Furthermore, we can also consider an identification of the extra dimensional space by Z_2 parity:

$$y \cong -y. \tag{2.6}$$

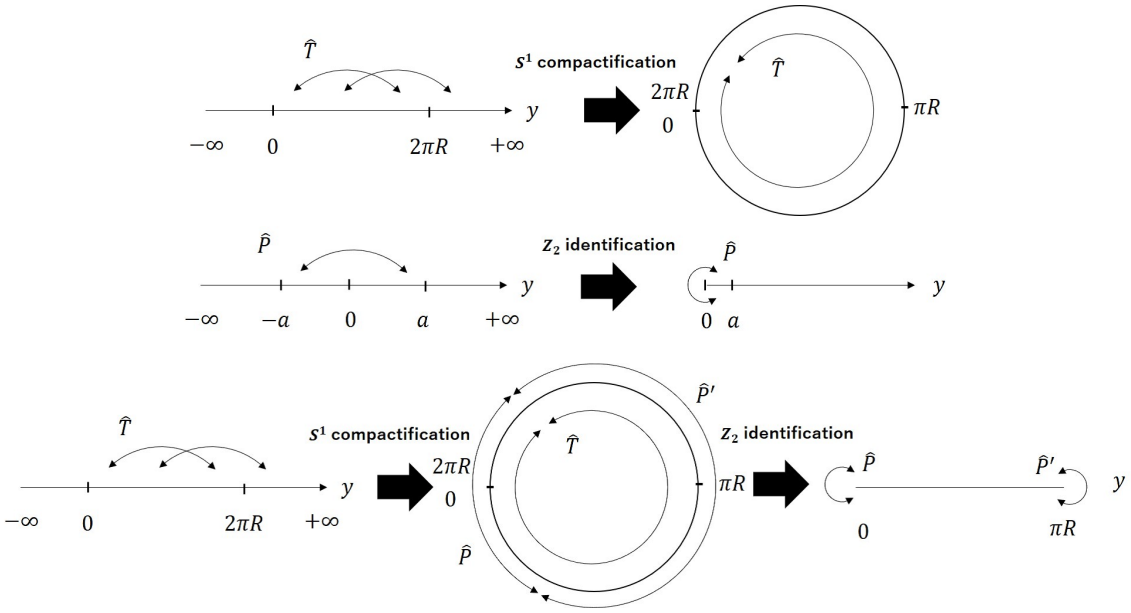

Figure 1: The upper, middle and lower figures show the S^1 compactification, the Z_2 identification and S^1/Z_2 orbifold, respectively. y denotes the extra-dimensional coordinate. $\hat{T}$ and $\hat{P}$ ($\hat{P}'$) are denote the operators of the $2\pi R$ transformation and the parity transformation at $y = 0$ ($y = \pi R$) boundary, respectively.

Imposing the Z_2 parity, the fundamental region of the extra dimensional space is the half-line $[0, \infty)$, that is, the theory has a boundary at $y = 0$. The boundary conditions of the vector field A_M and the fermion in the fundamental representation of the symmetry group at $y = 0$ are as follows.

$$\begin{aligned}
\hat{P}\left[\mathcal{A}_\mu(x,y)\right] &= P\mathcal{A}_\mu(x,y)P^\dagger = \mathcal{A}_\mu(x,-y), \\
\hat{P}\left[\mathcal{A}_y(x,y)\right] &= -P\mathcal{A}_y(x,y)P^\dagger = \mathcal{A}_y(x,-y), \\
\hat{P}\left[\Psi(x,y)\right] &= \pm P\gamma^5\Psi(x,y) = \Psi(x,-y),
\end{aligned} \tag{2.7}$$

where $\hat{P}$ is the parity operator around $y = 0$, whose eigenvalues are also ± 1 and P is the parity matrix. The signs for $\mathcal{A}_\mu$ and $\mathcal{A}_y$ in second line are derived from the parity invariance of the kinetic term $F_{MN}F^{MN}$. The matrix γ^5 indicates that the left-handed and the right-handed fermion have the opposite eigenvalue each other. Therefore, the five-dimensional fermion has no Dirac mass term $\overline{\Psi}\Psi$ because of the odd parity.

The S_1/Z_2 orbifold is a compactification operating Z_2 identification in addition to S^1 compactification. This leads to consider the extra dimension only in the range of $[0, \pi R]$, that is, the theory has the two boundaries at $y = 0$ and πR. Similarly, we can also consider the parity transformation around $y = \pi R$, whose operator is similarly to $y = 0$ case, $\hat{P}'$. Since these three operators, $\hat{T}$, $\hat{P}$, $\hat{P}'$ satisfy the relation $\hat{T} = \hat{P}\hat{P}'$ as shown in

Fig. 1, the fields are classified by the eigenvalues of $\hat{P}$ and $\hat{P}'$:

$$(\hat{P},\hat{P}') = \begin{cases} (+1,+1) : \hat{T} = +1 \\ (+1,-1) : \hat{T} = -1 \\ (-1,+1) : \hat{T} = -1 \\ (-1,-1) : \hat{T} = +1 \end{cases} . \tag{2.8}$$

By this classification, the wave functions can be expanded by the plane waves, which is called Kaluza-Klein (KK) expansion. For the scalar field Φ, KK expansion is carried out as follows.

$$\Phi(x,y) = \begin{cases} \frac{1}{\sqrt{2\pi R}}\phi^{(0)}(x) + \sum_{n=1}^{\infty}\frac{1}{\sqrt{\pi R}}\cos\left(\frac{n}{R}y\right)\phi^{(n)}(x) & : (+1,+1) \\ \frac{1}{\sqrt{2\pi R}}\phi^{(0)}(x) + \sum_{n=1}^{\infty}\frac{1}{\sqrt{\pi R}}\cos\left(\frac{n+1/2}{R}y\right)\phi^{(n)}(x) & : (+1,-1) \\ \frac{1}{\sqrt{2\pi R}}\phi^{(0)}(x) + \sum_{n=1}^{\infty}\frac{1}{\sqrt{\pi R}}\sin\left(\frac{n+1/2}{R}y\right)\phi^{(n)}(x) & : (-1,+1) \\ \sum_{n=1}^{\infty}\frac{1}{\sqrt{\pi R}}\sin\left(\frac{n}{R}y\right)\phi^{(n)}(x) & : (-1,-1) \end{cases} , \tag{2.9}$$

where $\phi^{(n)}(x)$ are four dimensional fields and called as the n-th KK fields. Once the wave function in extra dimensional space are found, four-dimensional physical quantities can be evaluated through the integral of the extra dimensional space. Especially, the mass term in four dimension is given by.

$$\int d^4x dy\, \mathcal{L}_5(x,y) \supset \int d^4x dy\, (\partial_5\Phi(x,y))^2 = -\int d^4x \sum_n \left(\frac{n+\nu}{R}\right)^2 \phi^{(n)}(x)^2, \tag{2.10}$$

where $\nu = 0$ $(1/2)$ for $\hat{T} = 1$ (-1), respectively. This equation means that the extra dimensional momentum is identified with the mass in four-dimensional low energy theory. R^{-1} is called as the compactification scale, which is a typical energy scale specifying the physical effects of the extra dimensions. When the energy scale of the theory is smaller than R^{-1}, the radius R is small and can be regarded as internal degree of freedom, that is the dimension of the theory is approximately four. In constructing the model, R^{-1} is larger than TeV scale because no new particle have been discovered in the present collider experiments. In the low energy theory where the energy scale E is much smaller than R^{-1}, $E \ll R^{-1}$, we have only to consider the light state with the mass $m \ll 1/R$, thai is, only KK zero mode with the parities $(\hat{P},\hat{P}') = (+1,+1)$ because only these states have the massless state as shown in Fig. 2.

2.2 Simplest $SU(6)$ gGHU

In this subsection, we review the simplest $SU(6)$ gGHU shown in [8].

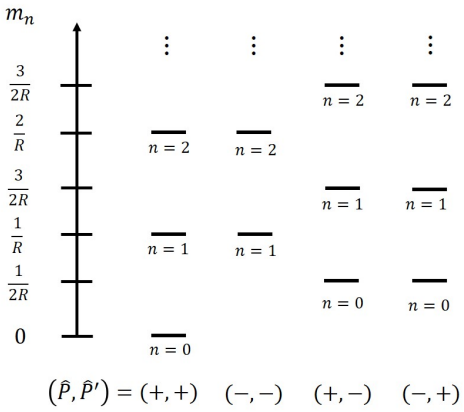

Figure 2: Kaluza-Klein masses with the parities $(\hat{P}, \hat{P}')$.

2.2.1 Parity conditions

We consider an $SU(6)$ grand Gauge-Higgs unification on S^1/Z_2 orbifold. The five-dimensional lagrangian of the gauge field is given by

$$\mathcal{L}_{5,g} = -\frac{1}{4}\mathcal{F}^a_{MN}\mathcal{F}^{a,MN}, \qquad (a = 1, 2, ..., 34, 35) \tag{2.11}$$

where the field strength tensor is given by $F^a_{MN} = \partial_M \mathcal{A}^a_N - \partial_N \mathcal{A}^a_M + i f^{abc} A^b_M A^c_N$, and f^{abc} is the structure constant of $SU(6)$. The parity matrices at each fixed point are

$$\begin{cases} P = \mathrm{diag}(-1,-1,-1,-1,-1,+1) \\ P' = \mathrm{diag}(-1,-1,+1,+1,+1,+1) \end{cases} . \tag{2.12}$$

According to Eq. (2.7), the eigenvalues for each components of four-dimensional gauge field are found

$$(\hat{P}, \hat{P}')_{\mathcal{A}_\mu} = \left(\begin{array}{cc|ccc|c} (+,+) & (+,+) & (+,-) & (+,-) & (+,-) & (-,-) \\ (+,+) & (+,+) & (+,-) & (+,-) & (+,-) & (-,-) \\ \hline (+,-) & (+,-) & (+,+) & (+,+) & (+,+) & (-,+) \\ (+,-) & (+,-) & (+,+) & (+,+) & (+,+) & (-,+) \\ (+,-) & (+,-) & (+,+) & (+,+) & (+,+) & (-,+) \\ \hline (-,-) & (-,-) & (-,+) & (-,+) & (-,+) & (+,+) \end{array}\right) . \tag{2.13}$$

On the boundary $y = 0$ and πR, the states imposed by the Neumann boundary condition survive. Therefore, the gauge symmetry on the boundaries are $SU(5) \times U(1)_X$ $(y = 0)$ and $SU(2)_L \times SU(4) \times U(1)$ $(y = \pi R)$. Comparing the gauge symmetry of the standard model, $U(1)_X$ symmetry is extra because the SM gauge symmetries are contained in $SU(5)$ gauge symmetry: $SU(5) \supset SU(3)_C \times SU(2)_L \times U(1)_Y$. In this thesis, this gauge symmetry is assumed to be broken by some mechanism, for example, the four dimensional scalar field

and its potential are introduced to $y = 0$ boundary and this symmetry is broken by the vacuum expectation value (VEV) of the scalar fields. After the $U(1)_X$ gauge symmetry is spontaneously broken, the remaining gauge symmetries on the boundaries are given by

$$\begin{aligned} &SU(5) && : y = 0, \\ &SU(3)_C \times SU(2)_L \times U(1)_Y && : y = \pi R. \end{aligned} \tag{2.14}$$

Since only the KK zero mode with $(+,+)$ are massless, the gauge symmetry in this theory is broken by S^1/Z_2 orbifold

$$SU(6) \to SU(3)_C \times SU(2)_L \times U(1)_Y \times U(1)_X \to SU(3)_C \times SU(2)_L \times U(1)_Y. \tag{2.15}$$

Similarly, according to Eq. (2.7) the eigenvalues for each components of an extra dimensional gauge field are

$$(\hat{P}, \hat{P}')_{\mathcal{A}_y} = \left(\begin{array}{cc|ccc|c} (-,-) & (-,-) & (-,+) & (-,+) & (-,+) & (+,+) \\ (-,-) & (-,-) & (-,+) & (-,+) & (-,+) & (+,+) \\ \hline (-,+) & (-,+) & (-,-) & (-,-) & (-,-) & (+,-) \\ (-,+) & (-,+) & (-,-) & (-,-) & (-,-) & (+,-) \\ (-,+) & (-,+) & (-,-) & (-,-) & (-,-) & (+,-) \\ \hline (+,+) & (+,+) & (+,-) & (+,-) & (+,-) & (-,-) \end{array}\right). \tag{2.16}$$

The massless fields are found

$$A_y^{(0)} = \frac{1}{\sqrt{2}} \left(\begin{array}{cc|ccc|c} 0 & 0 & 0 & 0 & 0 & A_y^{25(0)} - iA_y^{26(0)} \\ 0 & 0 & 0 & 0 & 0 & A_y^{27(0)} - iA_y^{28(0)} \\ \hline 0 & 0 & 0 & 0 & 0 & 0 \\ 0 & 0 & 0 & 0 & 0 & 0 \\ 0 & 0 & 0 & 0 & 0 & 0 \\ \hline A_y^{25(0)} + iA_y^{26(0)} & A_y^{27(0)} + iA_y^{28(0)} & 0 & 0 & 0 & 0 \end{array}\right). \tag{2.17}$$

where $A_y^{(0)}$ is the KK zero mode of $\mathcal{A}_y$. They behave like the SM Higgs fields under the gauge symmetries shown in Eq. (2.15), so that we can identify them with the components of the Higgs field

$$H \equiv \frac{1}{\sqrt{2}} \begin{pmatrix} A_y^{25(0)} - iA_y^{26(0)} \\ A_y^{27(0)} - iA_y^{28(0)} \end{pmatrix}. \tag{2.18}$$

In this setup, the doublet-triplet splitting problem is solved by the orbifolding since the colored Higgs has the parities $(+,-)$ and become massive [13].

In this thesis, the VEV of the Higgs field is parametrized as

$$\left\langle A_y^a \right\rangle = \frac{2\alpha}{g_5 R} \delta_{28}^a, \tag{2.19}$$

where α is a dimensionless parameter. Note that the KK fields have the masses originated from the Higgs VEV and the extra dimensional momentum, their masses are found to be

$$m_n^2 = \frac{(n + \nu \pm q\alpha)^2}{R^2}, \tag{2.20}$$

where q an the integer defined by the $SU(2)$ representation of the fields. In particular, the W boson mass is given by,

$$m_W = \frac{\alpha}{R}. \tag{2.21}$$

2.2.2 Effective potential

The electroweak symmetry breaking occur by the Higgs field with the nontrivial VEV. In GHU, since the Higgs fields is originated from the gauge fields, the Higgs potential at tree level is protected by five-dimensional gauge symmetry. Therefore, the Higgs potential arises from quantum corrections. The potential is generated at one-loop by Coleman-Weinberg mechanism,

$$V(q\alpha) = \sum_n (\pm g) \int \frac{d^4 p_E}{(2\pi)^4} \log[p_E^2 + m_n^2] = g\mathcal{F}^{\pm}(q\alpha), \tag{2.22}$$

with

$$\mathcal{F}^{\pm}(q\alpha) = \pm \sum_n \int \frac{d^4 p_E}{(2\pi)^4} \log[p_E^2 + m_n^2], \tag{2.23}$$

where the overall sign $+(-)$ stands for fermion (boson) contribution, respectively. g means the spin degree of freedom of the field running in the loop. The loop momentum p_E is taken to be Euclidean. The potential $\mathcal{F}$ depends on the mass spectrum of KK-fields m_n, which is classified depending on the mass spectra as follows.

$$\begin{aligned} \mathcal{F}^{\pm}(q\alpha) &= \mp \frac{3}{64\pi^6 R^4} \sum_{k=1}^{\infty} \frac{\cos(2\pi q\alpha k)}{k^5} && : m_n^2 = \frac{(n+\alpha)^2}{R^2}, \\ \mathcal{F}^{\pm}_{1/2}(q\alpha) &= \mp \frac{3}{64\pi^6 R^4} \sum_{k=1}^{\infty} (-1)^k \frac{\cos(2\pi q\alpha k)}{k^5} && : m_n^2 = \frac{(n+1/2+\alpha)^2}{R^2}. \end{aligned} \tag{2.24}$$

When a VEV is obtained from the Higgs potential, whether the symmetry breaking occurs can be determined by the product of the Wilson line W and the unitary matrix corresponding to the transformational operator $T = PP'$,

$$\hat{W} = W \times T = \mathcal{P} \exp\left\{ ig_5 \int_0^{2\pi R} dy \, \langle A_5 \rangle \right\} \times PP', \tag{2.25}$$

which is discussed in appendix B. This product and the generator for remaining symmetry after getting a VEV, T^a are commutative:

$$[\hat{W}, T^a] = [T^a, \hat{W}] = 0. \tag{2.26}$$

In this model at $\alpha = 0$ case, remaining gauge symmetries in the low energy scale are $SU(3)_C \times SU(2)_L \times U(1)_Y$ shown in Eq. (2.15), which correspond to the generators of $SU(6)$ gauge group, $T^{8,13,14,15,20,21,22,23}$, $T^{1,2,3}$ and T^{24}, respectively. At $\alpha = 1/2$ case, $T^{8,13,14,15,20,21,22,23}$, T^3 and T^{24} are commutative with the product shown in Eq. (2.25), thus the remaining symmetries are $SU(3)_C \times U(1) \times U(1)_Y$. Furthermore, at $\alpha \neq 0, 1/2$ case, T^3 and T^{24} cannot be commutative with the product, but the linear combination $T^3 + \sqrt{5/3}T^{24}$ is commutative, so that the remaining symmetry is $SU(3)_C \times U(1)_{EM}$. Therefore, the condition that the electroweak symmetry breaking occurs is

$$0 < \alpha < 1/2. \tag{2.27}$$

The Weinberg angle is the same as the Georgi-Glashow $SU(5)$ GUT,

$$\sin^2 \theta_W = \frac{5/3}{5/3 + 1} = \frac{3}{8}. \tag{2.28}$$

2.2.3 Simplest model

We discussed mainly the boson part of gGHU. We now discuss the fermion part and introduce the simplest embedding of the quarks and leptons into five-dimensional fields.

In embedding the quarks and leptons into the fermions in the bulk, they must be zero-mode of KK fields since the quarks and leptons should be massless before the Higgs field has the VEV. Noting their chiralities, the quarks and leptons in one generation can be embedded into two **6** and one **20** representations without exotic states in zero mode sector:

$$\begin{aligned}
\overline{\mathbf{6}} &= \begin{cases} \overline{\mathbf{6}}_L &= (\overline{\mathbf{3}}, \mathbf{1})^{(+,-)}_{1/3,-1} \oplus l_L(\mathbf{1}, \mathbf{2})^{(+,+)}_{-1/2,-1} \oplus (\mathbf{1}, \mathbf{1})^{(-,-)}_{0,5} \\ \overline{\mathbf{6}}_R &= (\overline{\mathbf{3}}, \mathbf{1})^{(-,+)}_{1/3,-1} \oplus (\mathbf{1}, \mathbf{2})^{(-,-)}_{-1/2,-1} \oplus \nu_R(\mathbf{1}, \mathbf{1})^{(+,+)}_{0,5} \end{cases}, \\
\overline{\mathbf{6}} &= \begin{cases} \overline{\mathbf{6}}_L &= (\overline{\mathbf{3}}, \mathbf{1})^{(-,-)}_{1/3,-1} \oplus (\mathbf{1}, \mathbf{2})^{(-,+)}_{-1/2,-1} \oplus (\mathbf{1}, \mathbf{1})^{(+,-)}_{0,5} \\ \overline{\mathbf{6}}_R &= d^*_R(\overline{\mathbf{3}}, \mathbf{1})^{(+,+)}_{1/3,-1} \oplus (\mathbf{1}, \mathbf{2})^{(+,-)}_{-1/2,-1} \oplus (\mathbf{1}, \mathbf{1})^{(-,+)}_{0,5} \end{cases}, \\
\mathbf{20} &= \begin{cases} \mathbf{20}_L = & q_L(\mathbf{3}, \mathbf{2})^{(+,+)}_{1/6,-3} \oplus (\overline{\mathbf{3}}, \mathbf{1})^{(+,-)}_{-2/3,-3} \oplus (\mathbf{1}, \mathbf{1})^{(+,-)}_{1,-3} \\ & \oplus (\overline{\mathbf{3}}, \mathbf{2})^{(-,+)}_{-1/6,3} \oplus (\mathbf{3}, \mathbf{1})^{(-,-)}_{2/3,3} \oplus (\mathbf{1}, \mathbf{1})^{(-,-)}_{-1,3} \\ \mathbf{20}_R = & (\mathbf{3}, \mathbf{2})^{(-,-)}_{1/6,-3} \oplus (\overline{\mathbf{3}}, \mathbf{1})^{(-,+)}_{-2/3,-3} \oplus (\mathbf{1}, \mathbf{1})^{(-,+)}_{1,-3} \\ & \oplus (\overline{\mathbf{3}}, \mathbf{2})^{(+,-)}_{-1/6,3} \oplus u_R(\mathbf{3}, \mathbf{1})^{(+,+)}_{2/3,3} \oplus e_R(\mathbf{1}, \mathbf{1})^{(+,+)}_{-1,3} \end{cases}, \end{aligned} \tag{2.29}$$

where, in $(q_1, q_2)^{(s_1,s_2)}_{r_1,r_2}$, q_1, q_2, r_1 and r_2 are the representation under $SU(3)_C$, $SU(2)_L$, $U(1)_Y$ and $U(1)_X$, respectively, and (s_1, s_2) is the sets of the parities on the $y = 0$ and πR.

Unfortunately, the down-type and the charged lepton Yukawa couplings which is generated from the gauge interaction in GHU, are not allowed in this embedding since the left-handed $SU(2)_L$ doublets (q_L and l_L) and the right-handed $SU(2)_L$ singlets (d_R and e_R) are embedded into different $SU(6)$ multiplet. This problem seems to be persistent as long as the quarks and leptons are embedded into five-dimensional fields. Therefore, we must consider other embeddings of the SM fermions allowing all of the Yukawa couplings.

3 Fermion mass hierarchy in gGHU

In this section, $SU(6)$ grand Gauge-Higgs unification with the bulk fermions and the localized kinetic terms is discussed. At the end of section 2, we saw that the standard model fermions embedded into five-dimensional field can not allow the down-type and the charged lepton Yukawa couplings. Therefore, we have to propose a different way of embedding reproducing all of Yukawa couplings. In the first half of this section, we introduce the bulk and mirror fermions to reproduce the Yukawa couplings. The quarks and leptons are introduced at $y = 0$ boundary. Yukawa couplings except for top quark can be reproduced through the propagation of the bulk fermions which couple to the quarks and leptons [1]. In the second half of this section, we introduce the localized gauge kinetic terms, which can enhance the SM fermion masses and help to obtain top quark mass. We obtain the suitable parameter region reproducing the masses of the SM fermions [2].

3.1 Fermion sector

3.1.1 Bulk and mirror fermion

We introduce the bulk fermions Ψ and the mirror $\tilde{\Psi}$ fermions. They are five-dimensional fields and have an opposite Z_2 parity each other. The reason of introducing mirror fermion as follows. In general, massless KK zero modes absent in the SM (referred to as exotic fermions) are generated from the bulk fields. Since the Dirac mass terms cannot be allowed in S^1/Z_2, we introduce the mirror fermion and the mass term with the bulk and the mirror fermions to give masses to massless exotic fermions.

$$\mathcal{L}_{\text{bulk+mirror}} = \overline{\Psi} i \not{D}_5 \Psi + \overline{\tilde{\Psi}} i \not{D}_5 \tilde{\Psi} + \frac{\lambda}{\pi R} \overline{\Psi} \tilde{\Psi} + \frac{\lambda}{\pi R} \overline{\tilde{\Psi}} \Psi, \tag{3.1}$$

where the bulk mass parameter λ is dimensionless. Denoting the mass eigenstates of n-th KK fields for the bulk and the mirror fermions $\psi^{(n)}$ and $\tilde{\psi}^{(n)}$, respectively, the kinetic term of n-th KK fields in the basis $(\psi^{(n)}, \tilde{\psi}^{(n)})$ can be expressed in the momentum space

$$K_{\psi^{(n)}} = \begin{pmatrix} \not{p} - m_n & \lambda/\pi R \\ \lambda/\pi R & \not{p} + m_n \end{pmatrix}, \tag{3.2}$$

Where m_n is KK mass in Eq. (2.10). The mass eigenstate can be obtained by diagonalizing of this matrix, and the corresponding eigenvalues are $\pm\sqrt{m_n^2 + (\lambda/\pi R)^2}$. Therefore, the massless exotic states can be avoided by the non-zero bulk mass λ. The propagator of the bulk and mirror fermions is given by

$$\Delta_{\psi^{(n)}} = i K^{-1}_{\psi^{(n)}} = \frac{i}{p^2 - m_n^2 - (\lambda/\pi R)^2} \begin{pmatrix} \not{p} + m_n & -\lambda/\pi R \\ -\lambda/\pi R & \not{p} - m_n \end{pmatrix}, \tag{3.3}$$

or in Euclidean form

$$\Delta^E_{\psi^{(n)}} = i\Delta_{\psi^{(n)}} = \frac{1}{p_E^2 + m_n^2 + (\lambda/\pi R)^2} \begin{pmatrix} i\not{p}_E - m_n & \lambda/\pi R \\ \lambda/\pi R & i\not{p}_E + m_n \end{pmatrix}, \tag{3.4}$$

where $\not{p}$ and $\not{p}_E$ are the momentum contracted by the gamma matrices γ^μ in Minkowski and Euclid frame, respectively.

3.1.2 Fermion mass hierarchy

The quarks and leptons are embedded into $SU(5)$ multiplets localized at $y = 0$ boundary, which are three sets of decuplet, anti-quintet and singlet χ_{10}, $\chi_{\overline{5}}$ and χ_1, respectively. We also introduce three types of the bulk and mirror fermions shown in Table 1-4. In order to realize the quark and lepton masses, the interactions between the bulk fermion and the boundary localized fermions are necessary. To allow such masses, we have to choose appropriate $SU(6)$ representations for the bulk fermions carefully. Note that the mirror fermions have no coupling to quarks and leptons. Table 2-4 shows the representations for the bulk and mirror fermions introduced in our model in addition to quarks and leptons, which corresponds to the matter content for one generation. Totally, three copies of them are present in this model.

Lagrangian of the fermions is given by

$$\begin{aligned}
\mathcal{L}_{\text{matter}} = & \sum_{a=20,15,6} \left[\overline{\Psi}_a i\Gamma^M D_M \Psi_a + \overline{\tilde{\Psi}}_a i\Gamma^M D_M \tilde{\Psi}_a + \left(\frac{\lambda_a}{\pi R} \overline{\Psi}_a \tilde{\Psi}_a + \text{ h.c.} \right) \right] \\
& + \delta(y) \left[\overline{\chi}_{10} i\Gamma^\mu D_\mu \chi_{10} + \overline{\chi}_{5^*} i\Gamma^\mu D_\mu \chi_{5^*} + \overline{\chi}_1 i\Gamma^\mu D_\mu \chi_1 \right. \\
& + \sqrt{\frac{2}{\pi R}} \left\{ \epsilon_{20} \left(\overline{\chi}_{10} \Psi_{10\subset 20} + \overline{\chi}^c_{10} \Psi_{10^*\subset 20} \right) + \epsilon_{15} \left(\overline{\chi}_{10} \Psi_{10\subset 15} + \overline{\chi}^c_{5^*} \Psi_{5\subset 15} \right) \right. \\
& \left. \left. + \epsilon_6 \left(\overline{\chi}_{5^*} \Psi_{5\subset 6} + \overline{\chi}_1 \Psi_{1\subset 6} \right) + \text{h.c.} \right\} \right].
\end{aligned}$$

The first line is Lagrangian for the bulk and mirror fermions, and the remaining terms are Lagrangian localized on $y = 0$ boundary. Note that the subscript "a" denotes the $SU(6)$ representations of the bulk and mirror fermions. The last two lines are mixing mass terms between the bulk fermions and the SM fermions. $\Psi_{M\subset N}$ is a bulk fermion for M in $SU(5)$ representation and N means $SU(6)$ representation. ϵ_i are the strength of the mixing term between the bulk fermion and the SM fermion. Note that all of the boundary terms respect $SU(5)$ symmetry structure.

After the extra-dimensional integral, the interaction term between one bulk fermion and one boundary fermion is obtained

$$\int dy \mathcal{L}_{\text{matter}} \supset \sum_n \frac{1}{\pi R} \left[\epsilon_L \overline{u}_L \psi^{(n)}_R + \epsilon_L \overline{u}_R \psi^{(n)}_L \right]. \tag{3.5}$$

bulk fermion $SU(6) \to SU(5)$	mirror fermion
$20^{(+,P_{20})} = 10 \oplus 10^*$	$20^{(-,-P_{20})}$
$15^{(+,P_{15})} = 10 \oplus 5$	$15^{(-,-P_{15})}$
$6^{(-,P_6)} = 5 \oplus 1$	$6^{(+,-P_6)}$

Table 1: Representation of bulk fermions and the corresponding mirror fermions. P_i are parity of bulk fermion for **i** representation in $SU(6)$ ($P_i = \pm 1$). R in $R^{(+,+)}$ means an $SU(6)$ representation of the bulk fermion. r_i in $r_1 \oplus r_2$ are $SU(5)$ representations.

bulk fermion $SU(5) \to SU(3)_C \times SU(2)_L \times U(1)_Y$	SM fermion coupling to bulk
$10 = Q_{20}(3,2)_{1/6}^{(+,P_{20})} \oplus U_{20}^*(3^*,1)_{-2/3}^{(+,-P_{20})} \oplus E_{20}^*(1,1)_1^{(+,-P_{20})}$	$q_L(3,2)_{1/6}, u_R^c(3^*,1)_{-2/3}, e_R^c(1,1)_1$
$10^* = Q_{20}^*(3^*,2)_{-1/6}^{(-,-P_{20})} \oplus U_{20}(3,1)_{2/3}^{(-,P_{20})} \oplus E_{20}(1,1)_{-1}^{(-,P_{20})}$	$q_L^c(3^*,2)_{-1/6}, u_R(3,1)_{2/3}, e_R(1,1)_{-1}$

Table 2: **20** bulk fermion and SM fermions per a generation. P_{20} is parity of bulk fermion for **20** ($P_{20} = \pm 1$). R in $R^{(+,+)}$ means an $SU(6)$ representation of the bulk fermion. $r_{1,2}$ in $(r_1, r_2)_a$ are $SU(3)$, $SU(2)$ representations in the SM, respectively. a is $\mathrm{U}(1)_Y$ charges.

bulk fermion $SU(5) \to SU(3)_C \times SU(2)_L \times U(1)_Y$	SM fermion coupling to bulk
$10 = Q_{15}(3,2)_{1/6}^{(+,-P_{15})} \oplus U_{15}^*(3^*,1)_{-2/3}^{(+,P_{15})} \oplus E_{15}^*(1,1)_1^{(+,P_{15})}$	$q_L(3,2)_{1/6}, u_R^c(3^*,1)_{-2/3}, e_R^c(1,1)_1$
$5 = D_{15}(3,1)_{-1/3}^{(-,P_{15})} \oplus L_{15}^*(1,2)_{1/2}^{(-,-P_{15})}$	$d_R(3,1)_{-1/3}, l_L^c(1,2)_{1/2}$

Table 3: **15** bulk fermion and SM fermions per a generation. P_{15} is parity of bulk fermion for **15** ($P_{15} = \pm 1$). $r_{1,2}$ in $(r_1, r_2)_a$ are $SU(3)$, $SU(2)$ representations in the SM, respectively. a is $\mathrm{U}(1)_Y$ charges.

bulk fermion $SU(5) \to SU(3)_C \times SU(2)_L \times U(1)_Y$	SM fermion coupling to bulk
$5 = D_6(3,1)_{-1/3}^{(-,-P_6)} \oplus L_6^*(1,2)_{1/2}^{(-,P_6)}$	$d_R(3,1)_{-1/3}, l_L^c(1,2)_{1/2}$
$1 = N_6^*(1,1)_0^{(+,-P_6)}$	$\nu_R^c(1,1)_0$

Table 4: **6** bulk fermion and SM fermions per a generation. P_6 is parity of bulk fermion for **6** ($P_6 = \pm 1$). $r_{1,2}$ in $(r_1, r_2)_a$ are $SU(3)$, $SU(2)$ representations in the SM, respectively. a is $\mathrm{U}(1)_Y$ charges.

The quark and lepton masses are generated from this interaction term, and the quadratic term of the SM fermions from this interaction at tree-level is given by

$$-i\overline{u}_L \not{p}_E Z_L u_L - i\overline{u}_R \not{p}_E Z_R u_R + (\overline{u}_L M u_R + \text{h.c.}), \tag{3.6}$$

with

$$\begin{aligned} \not{p}_E Z_L P_L &= \frac{-i}{\pi^2 R^2} \sum_n \epsilon_L \epsilon_L^* P_R \left\langle \psi^{(n)} \overline{\psi}^{(n)} \right\rangle_E P_L, \\ \not{p}_E Z_R P_R &= \frac{-i}{\pi^2 R^2} \sum_n \epsilon_R \epsilon_R^* P_L \left\langle \psi^{(n)} \overline{\psi}^{(n)} \right\rangle_E P_R, \\ M P_R &= \frac{1}{\pi^2 R^2} \sum_n \epsilon_L \epsilon_R^* P_R \left\langle \psi^{(n)} \overline{\psi}^{(n)} \right\rangle_E P_R, \end{aligned} \tag{3.7}$$

where the bulk fermion propagator $\left\langle \psi^{(n)}\overline{\psi}^{(n)} \right\rangle_E$ is (1,1) component of $\Delta^E_{\psi^{(n)}}$ in Eq. (3.4). We can calculate the summation of the KK fields,

$$\begin{aligned}\sum_n \frac{i\not{p}_E - m_n}{p_E^2 + m_n^2 + (\lambda/\pi R)^2} =& i\not{p}_E \frac{1}{x^2+\lambda^2} \mathrm{Re} f_0^{(T)}\left(\sqrt{x^2+\lambda^2}, q\alpha\right) \\ &+ \frac{1}{\pi R}\mathrm{Im} f_0^{(T)}\left(\sqrt{x^2+\lambda^2}, q\alpha\right),\end{aligned} \tag{3.8}$$

where T is the eigenvalue of periodicity, ± 1, and x is the dimensionless momentum $\not{p}_E \pi R$. The functions $f_0^{(T)}$ are the bulk fermion propagator from $y=0$ to $y=0$ in the bulk, and given by

$$\begin{aligned} f_0^{(T)} =& \sum_n \frac{1}{x + i\pi(n+\nu+\alpha)} \\ =& \begin{cases} \coth(x+i\pi\alpha) & : T=+1 (\nu = 0) \\ \tanh(x+i\pi\alpha) & : T=-1 (\nu = 1/2) \end{cases}. \end{aligned} \tag{3.9}$$

Therefore, Eq. (3.7) is rewritten as

$$\begin{aligned} Z_L &= \frac{\epsilon_L \epsilon_L^*}{\sqrt{x^2+\lambda^2}} \mathrm{Re} f_0^{(T)}\left(\sqrt{x^2+\lambda^2}, q\alpha\right), \\ Z_R &= \frac{\epsilon_R \epsilon_R^*}{\sqrt{x^2+\lambda^2}} \mathrm{Re} f_0^{(T)}\left(\sqrt{x^2+\lambda^2}, q\alpha\right), \\ M &= \frac{\epsilon_L \epsilon_R^*}{\pi R} \mathrm{Im} f_0^{(T)}\left(\sqrt{x^2+\lambda^2}, q\alpha\right). \end{aligned} \tag{3.10}$$

Integrating out all bulk fermions and normalizing the kinetic term to be canonical, we obtain the physical mass for the quarks and leptons.

$$m^a_{\mathrm{phys}} = \frac{M^a}{\sqrt{Z_L^a Z_R^a}} \qquad (a = u, d, e, \nu), \tag{3.11}$$

where M^a and $Z^a_{L,R}$ are the summation of all M and $Z_{L,R}$ for corresponding bulk fermions. u, d, e and ν stand for up-type quark, down-type quark, charged lepton and neutrino.

In this model, these are explicitly given by

$$\begin{aligned} m^u &= \frac{\epsilon_{20}^2}{\pi R}\left[\mathrm{Im} f_0^{(P_{20})}(\sqrt{x^2+\lambda_{20}^2}, \alpha) + \mathrm{Im} f_0^{(-P_{20})}(\sqrt{x^2+\lambda_{20}^2}, \alpha)\right], \\ Z_L^u &= 1 + \frac{\epsilon_{20}^2}{\sqrt{x^2+\lambda_{20}^2}}\left[\mathrm{Re} f_0^{(P_{20})}(\sqrt{x^2+\lambda_{20}^2}, \alpha) + \mathrm{Re} f_0^{(-P_{20})}(\sqrt{x^2+\lambda_{20}^2}, \alpha)\right] \\ &\quad + \frac{\epsilon_{15}^2}{\sqrt{x^2+\lambda_{15}^2}} \mathrm{Re} f_0^{(-P_{15})}(\sqrt{x^2+\lambda_{15}^2}, 0), \\ Z_R^u &= 1 + \frac{\epsilon_{20}^2}{\sqrt{x^2+\lambda_{20}^2}}\left[\mathrm{Re} f_0^{(P_{20})}(\sqrt{x^2+\lambda_{20}^2}, \alpha) + \mathrm{Re} f_0^{(-P_{20})}(\sqrt{x^2+\lambda_{20}^2}, \alpha)\right] \\ &\quad + \frac{\epsilon_{15}^2}{\sqrt{x^2+\lambda_{15}^2}} \mathrm{Re} f_0^{(P_{15})}(\sqrt{x^2+\lambda_{15}^2}, 0), \end{aligned} \tag{3.12}$$

$$
\begin{aligned}
m^d &= \frac{\epsilon_{15}^2}{\pi R}\mathrm{Im} f_0^{(-P_{15})}(\sqrt{x^2+\lambda_{15}^2},\alpha),\\
Z_L^d &= 1+\frac{\epsilon_{20}^2}{\sqrt{x^2+\lambda_{20}^2}}\left[\mathrm{Re} f_0^{(P_{20})}(\sqrt{x^2+\lambda_{20}^2},0)+\mathrm{Re} f_0^{(-P_{20})}(\sqrt{x^2+\lambda_{20}^2},0)\right]\\
&\quad+\frac{\epsilon_{15}^2}{\sqrt{x^2+\lambda_{15}^2}}\mathrm{Re} f_0^{(-P_{15})}(\sqrt{x^2+\lambda_{15}^2},\alpha),\\
Z_R^d &= 1+\frac{\epsilon_{15}^2}{\sqrt{x^2+\lambda_{15}^2}}\mathrm{Re} f_0^{(-P_{15})}(\sqrt{x^2+\lambda_{15}^2},\alpha)+\frac{\epsilon_6^2}{\sqrt{x^2+\lambda_6^2}}\mathrm{Re} f_0^{(P_6)}(\sqrt{x^2+\lambda_6^2},0),
\end{aligned}
\tag{3.13}
$$

$$
\begin{aligned}
m^e &= \frac{\epsilon_{15}^2}{\pi R}\mathrm{Im} f_0^{(P_{15})}(\sqrt{x^2+\lambda_{15}^2},\alpha),\\
Z_L^e &= 1+\frac{\epsilon_{15}^2}{\sqrt{x^2+\lambda_{15}^2}}\mathrm{Re} f_0^{(P_{15})}(\sqrt{x^2+\lambda_{15}^2},\alpha)+\frac{\epsilon_6^2}{\sqrt{x^2+\lambda_6^2}}\mathrm{Re} f_0^{(-P_6)}(\sqrt{x^2+\lambda_6^2},0),\\
Z_R^e &= 1+\frac{\epsilon_{20}^2}{\sqrt{x^2+\lambda_{20}^2}}\left[\mathrm{Re} f_0^{(P_{20})}(\sqrt{x^2+\lambda_{20}^2},0)+\mathrm{Re} f_0^{(-P_{20})}(\sqrt{x^2+\lambda_{20}^2},0)\right]\\
&\quad+\frac{\epsilon_{15}^2}{\sqrt{x^2+\lambda_{15}^2}}\mathrm{Re} f_0^{(P_{15})}(\sqrt{x^2+\lambda_{15}^2},\alpha),
\end{aligned}
\tag{3.14}
$$

$$
\begin{aligned}
m^\nu &= \frac{\epsilon_6^2}{\pi R}\mathrm{Im} f_0^{(-P_6)}(\sqrt{x^2+\lambda_6^2},\alpha),\\
Z_L^\nu &= 1+\frac{\epsilon_{15}^2}{\sqrt{x^2+\lambda_{15}^2}}\mathrm{Re} f_0^{(P_{15})}(\sqrt{x^2+\lambda_{15}^2},0)+\frac{\epsilon_6^2}{\sqrt{x^2+\lambda_6^2}}\mathrm{Re} f_0^{(-P_6)}(\sqrt{x^2+\lambda_6^2},\alpha),\\
Z_R^\nu &= 1+\frac{\epsilon_6^2}{\sqrt{x^2+\lambda_6^2}}\mathrm{Re} f_0^{(-P_6)}(\sqrt{x^2+\lambda_6^2},\alpha).
\end{aligned}
\tag{3.15}
$$

In the case of $x \gg \lambda$, the physical mass in Eq. (3.11) is approximated as

$$
m_{\mathrm{phys}}^a \sim \frac{\alpha}{R}e^{-\lambda} = m_W e^{-\lambda}. \tag{3.16}
$$

where $m_W = \alpha/R$ in Eq. (2.21) is used. Since the fermion mass generating this mechanism has an upper bound m_W, the top quark mass cannot be reproduced. Therefore, we consider some mechanism to enhance the fermion mass. Next subsection, we discuss that this problem is solved by deforming the mass spectrum of the gauge field.

3.2 Localized gauge kinetic terms

In the previous subsection, we discussed that the quark and lepton masses are generated by propagation of the bulk fermions. However, the top quark mass cannot be reproduced. We have to consider some mechanism to enhance it. From Eq. (3.16) the physical mass is proportional to α/R. Therefore, if the mass spectrum of the gauge boson is deforming

by some mechanism and the weak boson mass becomes $m_W \sim C^{-1} \times \alpha/R$, the physical mass is corrected as

$$m_{\rm phys} \sim C m_W e^{-\lambda}. \tag{3.17}$$

C must be larger than two to reproduce the top quark mass.

In this subsection, we consider introducing the localized gauge kinetic terms to obtain the enhancement factor C [2]. Lagrangian for $SU(6)$ gauge field including the localized terms is

$$\mathcal{L} = -\frac{1}{4}\mathcal{F}^{a,MN}\mathcal{F}^a_{MN} - 2\pi R c_1 \delta(y)\mathcal{F}^{b,\mu\nu}\frac{1}{4}\mathcal{F}^b_{\mu\nu} - 2\pi R c_2 \delta(y-\pi R)\frac{1}{4}\mathcal{F}^{c,\mu\nu}\mathcal{F}^c_{\mu\nu}, \tag{3.18}$$

where the first term is the gauge kinetic term in the bulk and $M,\ N = 0,1,2,3,5$. The second and third terms are the gauge kinetic terms localized at fixed points, and μ, $\nu = 0,1,2,3$. $c_{1,2}$ are dimensionless free parameters. The superscript a, b and c denote the gauge indices for $SU(6)$, $SU(5)$ and $SU(3)_C \times SU(2)_L \times U(1)_Y$, respecting the unbroken gauge symmetries in Eq. (2.14).

3.2.1 Mass spectrum

Introducing the localized gauge kinetic terms, the mass spectrum of the gauge field is modified. In general, the KK-expansion is given by

$$\mathcal{A}^\mu(x,y) = \sum_n f_n(y) A^\mu_n(x). \tag{3.19}$$

The wave functions satisfy a condition $f_n(y+\pi R) = e^{2i\pi(q\alpha+\nu)} f_n(y)$, where ν is the periodicity or $\nu = 0$ $(1/2)$ in periodic (anti-periodic) sector. Moreover, the wave function in the same basis satisfy the equation

$$\left[\partial_y^2 + m_n^2\left(1 + 2\pi R c_1 \delta(y) + 2\pi R c_2 \delta(y-\pi R)\right)\right] f_n(y) = 0, \tag{3.20}$$

where m_n is the KK mass in Eq. (2.20). Solving first this equation without delta function terms, the solutions of the wave function are given by

$$f_n(y) = \mathcal{N}_n \begin{cases} \cos(m_n y) + \beta_n^- \sin(m_n y)\,,\ y \in [-\pi R, 0] \\ \cos(m_n y) - \beta_n^+ \sin(m_n y)\,,\ y \in [0, \pi R], \end{cases} \tag{3.21}$$

where $\mathcal{N}_n$ is a normalization factor determined by $\int |f_n|^2 dy = 1$. $\beta_n^\pm$ and m_n can be determined by the continuity conditions at $y = 0,\ \pi R$ and the boundary conditions:

$$\beta_n^\pm = e^{\pm i\pi(q\alpha+\nu)} \sec(\pi(q\alpha+\nu))\xi_n c_1 \mp i \tan(\pi(q\alpha+\nu)) \cot\xi_n, \tag{3.22}$$

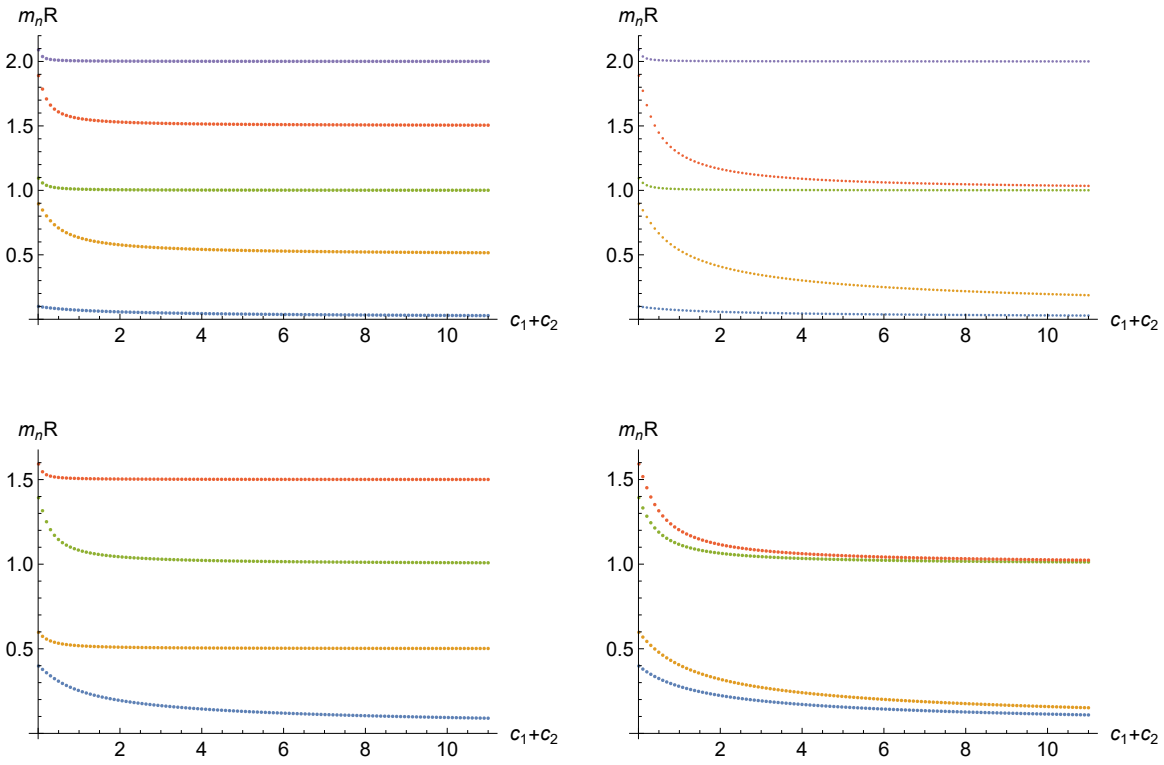

Figure 3: The mass spectra with $(q, \alpha) = (1, 0.1)$, which are solutions of Eq.(3.24), normalized by the compactification scale R^{-1} in the range of $0 \leq c_1 + c_2 \leq 11$. The upper figures show the mass spectra of the periodic fields ($\nu = 0$) with $r \equiv c_1/(c_1 + c_2) = 0, 1$ (left) and $r = 1/2$ (right). The lower figures show the mass spectra of the anti-periodic fields ($\nu = 1/2$) with $r = 0, 1$ (left) and $r = 1/2$ (right).

$$2\left(1 - c_1 c_2 \xi_n^2\right) \sin^2 \xi_n + (c_1 + c_2)\, \xi_n \sin 2\xi_n - 2\sin^2(\pi(q\alpha + \nu)) = 0, \tag{3.23}$$

where $\xi_n = \pi R m_n$

Since m_0 is around weak scale ($\sim$ 100 GeV) and $1/R$ is larger than 1 TeV, it is reasonable to suppose $\xi_0 \ll 1$. The mass of zero-th KK field in this limit is obtained by

$$\xi_0 \sim \frac{\sin(\pi(q\alpha + \nu))}{\sqrt{1 + c_1 + c_2}}. \tag{3.24}$$

For instance, the W boson is the gauge boson whose q and ν are 1 and 0, respectively, so that the W boson mass is given by

$$m_W \sim \frac{\sin(\pi\alpha)}{\pi R\sqrt{1 + c_1 + c_2}}. \tag{3.25}$$

Therefore, we can obtain the enhancement factor,

$$C = \frac{\alpha/R}{m_W} \sim \frac{\pi\alpha\sqrt{1 + c_1 + c_2}}{\sin(\pi\alpha)} \sim \sqrt{1 + c_1 + c_2}. \tag{3.26}$$

The mass spectrum given by Eq. (3.23) is shown in Fig. 3. This figure indicates that the mass spectra have the limited value at large c_1 and c_2. This values can be evaluated

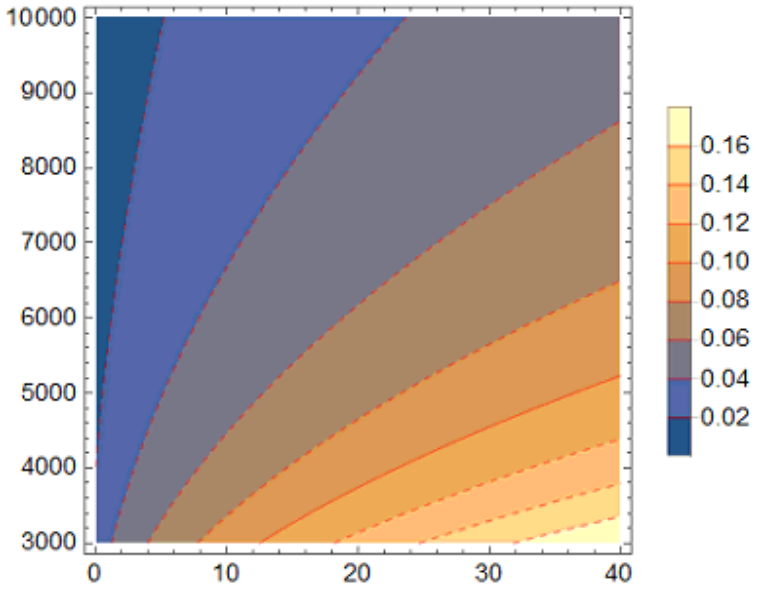

Figure 4: Higgs VEV α in the range $0 \leq c_1 + c_2 \leq 40$ (horizontal axis) and 3000 GeV $\leq 1/R \leq 10000$ GeV (vertical axis).

by Eq. (3.23). In the case of only one localized parameter $r = c_1/(c_1 + c_2) = 0$ or 1, the mass spectrum tends to be integer and half-integer KK mass,

$$\begin{aligned} \frac{n+\nu+\alpha}{R} &\to \frac{n+\nu}{R}, \\ \frac{n+\nu}{R}, \frac{n+\nu-\alpha}{R} &\to \frac{n+\nu-1/2}{R}. \end{aligned} \tag{3.27}$$

Similarly, in the case of $r = 1/2$, the mass spectrum tends to be integer KK mass,

$$\begin{aligned} \frac{n+\nu+\alpha}{R} &\to \frac{n}{R}, \\ \frac{n+\nu}{R}, \frac{n+\nu-\alpha}{R} &\to \frac{n-1}{R}. \end{aligned} \tag{3.28}$$

Fig. 4 shows the Higgs VEV α obtained from Eq. (3.25) with $m_W = 80.3$ GeV. According to this figure, the condition $\alpha \ll 1$ is obtained when the compactification scale $1/R$ is lager than a few TeV. Since the masses of the weak boson in Eq. (3.25) and the SM fermions in Eq. (3.11) are proportional to α under this condition, the ratios between the SM fermion masses and the W boson mass are independent of α. Fig. 5 shows the bulk mass λ_{20} dependence on the ratio of W boson mass and the physical up-type mass $m^u_{\rm phys}$ given by Eq. (3.11). The localized term dependence on the maximum of the ratio is displayed in a range of $0 < c_1 + c_2 < 20$. To reproduce the top quark mass, $c_1 + c_2 > 4$ is required.

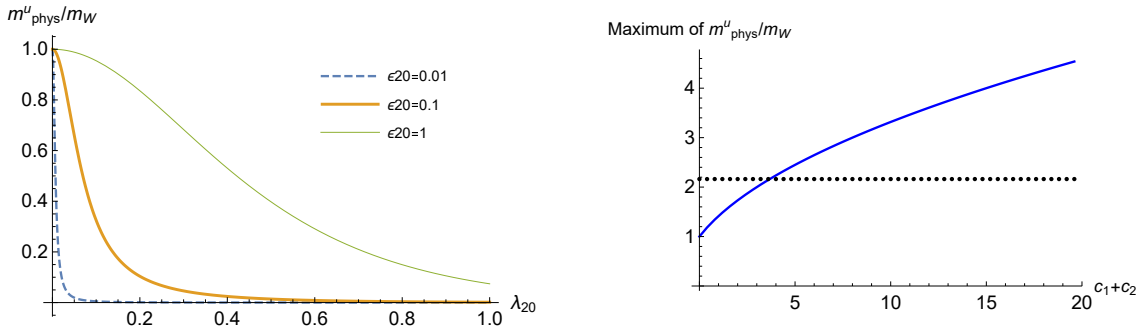

Figure 5: The bulk mass λ_{20} dependence on the ratio of the physical up-type mass and W boson mass $m^u_{\rm phys}/m_W$ with $c_1+c_2=0$ (left side) and the maximum ratio in the range of $0 \leq c_1+c_2 \leq 20$ (right side). Other parameters are taken to be 1. Dotted line means top quark mass: $m^u_{\rm phys}/m_W = m_{\rm top}/m_W \sim 2.15$.

3.2.2 Fermion mass hierarchy

We have to analyses the neutrino masses, prior to reproduce the value of the quark an lepton masses. Most of the neutrino masses are dominated by the contribution of **6** rep bulk fermion. Fig. 6 shows the λ_6 and ϵ_6 dependence of the neutrino mass, taking the other corresponding parameters as $c_1+c_2=10$, $\lambda_{15}=1$, $\epsilon_{15}=1$, $P_{15}=1$ and $P_6=1$. Since the neutrino masses are smaller than 1 eV, the suitable region is $m^\nu_{\rm phys}/m_W < 10^{-11}$ (blue region in Fig. 6). In this region, λ_6 is large ($\sim \mathcal{O}(10)$) or ϵ_6 is small ($< 10^{-4}$), and contribution of the representation **6** are exponentially small, so that the contribution can be ignored to reproduce the SM fermion masses except for SM neutrinos.

We have also to determine the parities of the **15** rep bulk fermion. Since the most of the down-type quark and charged lepton masses are dominated by the contribution of **15** rep bulk fermion, the ratios of down-type quark and charged lepton constrain the parities of the **15** rep bulk fermion. Fig. 7 shows λ_{15} dependence of the ratio, in the two cases:$P_{15}=\pm 1$, where other parameters are taken as $\epsilon_{15}=1$, $\lambda_{20}=1$ and $\epsilon_{20}=1$. According to this figure, the down-type quark mass is smaller (larger) than charged lepton mass in the case of $P_{15}=+1(-1)$. The experimental data tell as

$$\frac{m_{\rm down}}{m_{\rm electron}} \sim 9.1 > 1, \frac{m_{\rm strange}}{m_{\rm muon}} \sim 0.9 < 1, \frac{m_{\rm bottom}}{m_{\rm tauon}} \sim 2.3 > 1, \tag{3.29}$$

therefore the parity assignments of **15** representation for each generation have to be taken as

$$P_{15}^{\rm 1st} = -1, \qquad P_{15}^{\rm 2nd} = 1, \qquad P_{15}^{\rm 3rd} = -1. \tag{3.30}$$

Ignoring the contribution of **6** rep bulk fermions, the up-type quark, down-type quark and charged lepton are reproduced by the four parameters, λ_{20}, ϵ_{20}, λ_{15}, ϵ_{15}. Fig. 8 shows

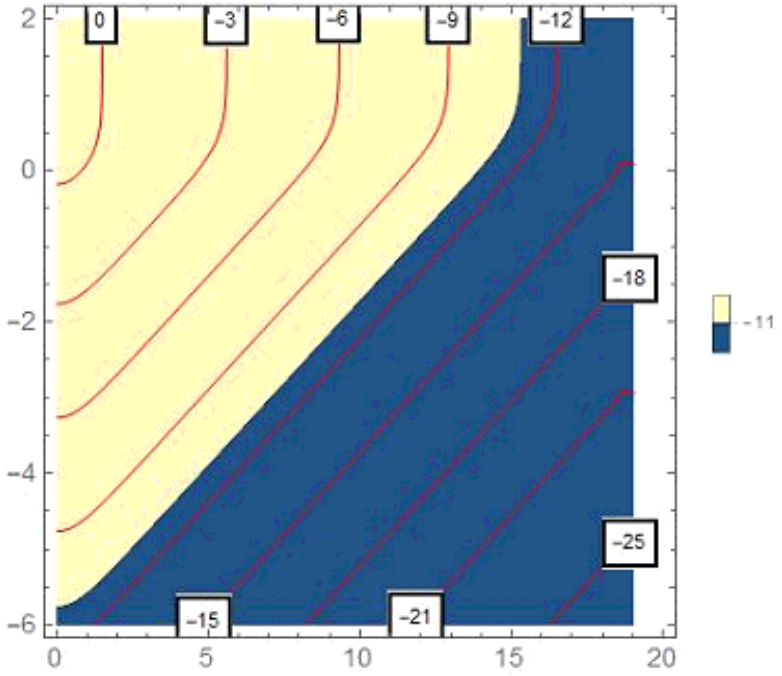

Figure 6: Common logarithms of the ratio of physical neutrino mass and W mass $m^{\nu}_{\rm phys}/m_W$. The vertical axis is $\log_{10}[\epsilon_6]$. The horizontal axis is λ_6. Parameters $c_1 + c_2$, λ_{15}, ϵ_{15}, P_{15} and P_6 are taken to be 10, 1, 1, 1 and 1, respectively. Red lines mean the order of magnitude for $m^{\nu}_{\rm phys}/m_W$. Blue region is an allowed region for neutrino mass.

the suitable parameters λ_{20}, λ_{15} and ϵ_{15} by changing the value of ϵ_{20} for each generations. We can find allowed parameter sets in a broad region. In the case of the first generation, the region lacking the data points appears around $\epsilon_{20} \sim 0.8$ since it is difficult to reproduce the mass hierarchy between the down quark and the electron, which is lager than those of the second and the third generation in Eq. (3.29). In the case of the second (third) generation, the region lacking the data point appears in that of $\epsilon_{20} < 0.05(0.6)$ since the up-type quark mass cannot be reproduced.

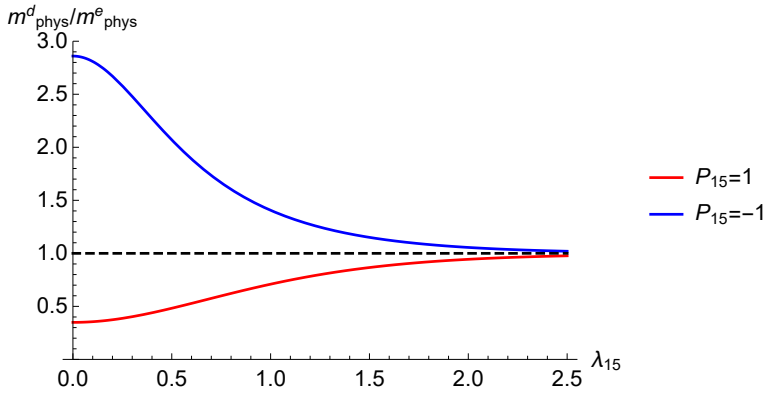

Figure 7: The ratio of the physical down-type mass and the physical charged lepton mass $m^d_{\rm phys}/m^e_{\rm phys}$. Parameters ϵ_{15}, λ_{20} and ϵ_{20} are taken to be 1.

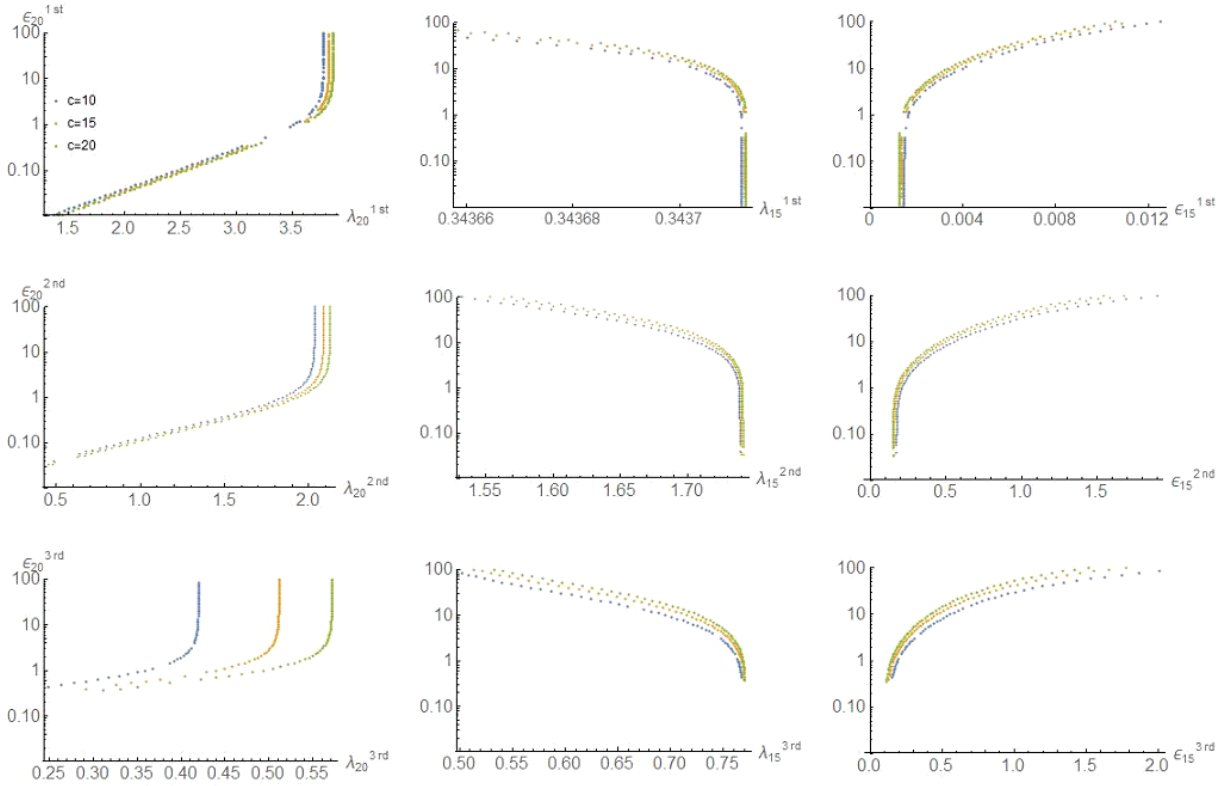

Figure 8: Scatter plots of the parameters reproducing the SM fermion masses except for neutrino masses. The upper, middle and bottom plots show ϵ_{20} dependence of λ_{20}, λ_{15} and ϵ_{15} for the first, the second and the third generation, respectively.

4 Flavor mixing angle in gGHU

In this section, the flavor mixing angle in $SU(6)$ gGHU is discussed. The flavor mixing angle is originated form the difference between the bases diagonalizing the SM fermion kinetic terms and the charged weak interactions. Unfortunately, the model discussed in the previous section has no mixing term of bose of the fermion kinetic term and the charged weak interaction. Therefore, we have to introduce the mixing of the bulk and boundary fermions to obtain the flavor mixing angle of the boundary fermions. In the first half of this section, we review the flavor mixing angle in SM. In the second half of this section, we improve the interaction of the bulk and boundary fermions. The number of the bulk fermions can be reduced and the flavor mixing angle can be reproduced.

4.1 Flavor mixing angle in Standard Model

When the Higgs VEV is absent, the interaction of the quarks and the Higgs fields H is given by Yukawa coupling

$$-Y^u_{ij}\overline{Q^I_{L,i}}Hd^I_{R,j} - Y^d_{ij}\overline{Q^I_{L,i}}\epsilon H^* u^I_{R,j}, \tag{4.1}$$

where $i,j = 1,2,3$ are the generation of the quarks, $Y^{u,d}_{ij}$ are the complex matrices and ϵ is 2×2 anti-symmetric tensor. This term can be diagonalized by the new basis $u_{L,R} = U^u_{L,R}u^I_{L,R}$ and $d_{L,R} = U^d_{L,R}d^I_{L,R}$, then we obtain the diagonal mass matrix of the quarks $M^{u,d}_{\rm diag} \equiv (v/2)U^{u,d}_L Y^{u,d} U^{u,d\,\dagger}_R = \mathrm{diag}(m^{u,d}_1, m^{u,d}_2, m^{u,d}_3)$, where m^u_i (m^d_i) is the mass of the i-th generation up(down)-type quark. Furthermore, the charged weak interaction terms can be rewritten by this basis,

$$-\frac{g}{\sqrt{2}}\overline{u^I_{L,i}}\gamma^\mu W^+_\mu d^I_{L,i} + \text{h.c.} = -\frac{g}{\sqrt{2}}\overline{u_{L,i}}\gamma^\mu W^+_\mu V_{\text{CKM}\,i,j} d_{L,j} + \text{h.c.}, \tag{4.2}$$

$$V_{\text{CKM}} \equiv U^u_L U^{d\,\dagger}_L. \tag{4.3}$$

V_{CKM} is Cabibbo-Kobayashi-Maskawa (CKM) matrix which is 3×3 unitary matrix. This matrix can be parameterized by three flavor mixing angles (θ_{12}, θ_{23}, θ_{31}) and the CP-violation phase δ. In this thesis, we choice the standard parametrization,

$$\begin{aligned} V_{\text{CKM}} &= \begin{pmatrix} 1 & 0 & 0 \\ 0 & c_{23} & s_{23} \\ 0 & -s_{23} & c_{23} \end{pmatrix} \begin{pmatrix} c_{13} & 0 & s_{13}e^{-i\delta} \\ 0 & 1 & 0 \\ -s_{13}e^{i\delta} & 0 & c_{13} \end{pmatrix} \begin{pmatrix} c_{12} & s_{12} & 0 \\ -s_{12} & c_{12} & 0 \\ 0 & 0 & 1 \end{pmatrix} \\ &= \begin{pmatrix} c_{12}c_{13} & s_{12}c_{13} & s_{13}e^{-i\delta} \\ -s_{12}c_{23} - c_{12}s_{23}s_{13}e^{i\delta} & c_{12}c_{23} - s_{12}s_{23}s_{13}e^{i\delta} & s_{23}c_{13} \\ s_{12}s_{23} - c_{12}c_{23}s_{13}e^{i\delta} & -c_{12}s_{23} - s_{12}c_{23}s_{13}e^{i\delta} & c_{23}c_{13} \end{pmatrix}, \end{aligned} \tag{4.4}$$

where s_{ij} and c_{ij} are $\sin\theta_{ij}$ and $\cos\theta_{ij}$, respectively.

4.2 Improving the interaction of the bulk and boundary fermion

In the previous model, the bulk fermions are introduced per generation. To reproduce the three flavor mixing angles and the CP phase, the interaction of the bulk and the boundary fermions must be modified [3]. We will discuss the case of one and two bulk fermions. For one bulk fermion case, we will find that massless SM fermions inevitably exist. Interaction with one bulk fermion and three generations of the boundary fermions is considered:

$$\begin{aligned}&\int dy \sum_{i=1}^{3} \delta(y) \sqrt{\frac{2}{\pi R}} \left(\epsilon_L^i \overline{\Psi} u_L^i + \epsilon_R^i \overline{\Psi} u_R^i + \text{h.c.}\right) \\ &\supset \sum_{i=1}^{3} \sum_n \frac{1}{\pi R} \left(\epsilon_L^i \overline{\psi}^{(n)} u_L^i + \epsilon_R^i \overline{\psi}^{(n)} u_R^i + \text{h.c.}\right).\end{aligned} \tag{4.5}$$

The contributions of this interaction to the wave function renormalization factors and mass of SM fermions are generated by integrating out the bulk fermion

$$\begin{aligned}Z_{L,R}^{ij} &= \frac{\epsilon_{L,R}^i \epsilon_{L,R}^{j*}}{\sqrt{x^2+\lambda^2}} \text{Re} f_0^{(T)} \left(\sqrt{x^2+\lambda^2}, q\alpha\right) \\ M^{ij} &= \frac{\epsilon_L^i \epsilon_R^{j*}}{\sqrt{x^2+\lambda^2}} \text{Im} f_0^{(T)} \left(\sqrt{x^2+\lambda^2}, q\alpha\right).\end{aligned} \tag{4.6}$$

However, since the mass term M^{ij} is proportional to the couplings $\epsilon^i \epsilon^{j*}$, the rank of M^{ij} is one, This fact indicates that two massless boundary fermions are remaining.

To solve this problem, one generation of the boundary fermions is located at $y = \pi R$ boundary. In this case, the interaction terms between the bulk and the SM fermions are modified

$$\begin{aligned}&\int dy \sum_{i=1}^{2} \delta(y) \sqrt{\frac{2}{\pi R}} \left(\epsilon_L^i \overline{\Psi} u_L^i + \epsilon_R^i \overline{\Psi} u_R^i + \text{h.c.}\right) \\ &\qquad + \delta(y-\pi R) \sqrt{\frac{2}{\pi R}} \left(\epsilon_L^3 \overline{\Psi} u_L^3 + \epsilon_R^3 \overline{\Psi} u_R^3 + \text{h.c.}\right) \\ &\supset \sum_{i=1}^{2} \sum_n \frac{1}{\pi R} \left(\epsilon_L^i \overline{\psi}^{(n)} u_L^i + \epsilon_R^i \overline{\psi}^{(n)} u_R^i + \text{h.c.}\right) \\ &\qquad + \sum_n \frac{1}{\pi R} (-1)^n \left(\epsilon_L^3 \overline{\psi}^{(n)} u_L^3 + \epsilon_R^3 \overline{\psi}^{(n)} u_R^3 + \text{h.c.}\right).\end{aligned} \tag{4.7}$$

Then, the corresponding wave function renormalization factors and masses are obtained

$$
\begin{aligned}
Z_{L,R} &= \frac{1}{\sqrt{x^2+\lambda^2}} \begin{pmatrix} \epsilon^1_{L,R}\epsilon^{1*}_{L,R}\mathrm{Re}f_0^{(T)} & \epsilon^1_{L,R}\epsilon^{2*}_{L,R}\mathrm{Re}f_0^{(T)} & \epsilon^1_{L,R}\epsilon^{3*}_{L,R}\mathrm{Re}f_1^{(T)} \\ \epsilon^2_{L,R}\epsilon^{1*}_{L,R}\mathrm{Re}f_0^{(T)} & \epsilon^2_{L,R}\epsilon^{2*}_{L,R}\mathrm{Re}f_0^{(T)} & \epsilon^2_{L,R}\epsilon^{3*}_{L,R}\mathrm{Re}f_1^{(T)} \\ \epsilon^3_{L,R}\epsilon^{1*}_{L,R}\mathrm{Re}f_1^{(T)} & \epsilon^3_{L,R}\epsilon^{2*}_{L,R}\mathrm{Re}f_1^{(T)} & \epsilon^3_{L,R}\epsilon^{3*}_{L,R}\mathrm{Re}f_0^{(T)} \end{pmatrix} \\
M &= \frac{1}{\sqrt{x^2+\lambda^2}} \begin{pmatrix} \epsilon^1_{L}\epsilon^{1*}_{R}\mathrm{Im}f_0^{(T)} & \epsilon^1_{L}\epsilon^{2*}_{R}\mathrm{Im}f_0^{(T)} & \epsilon^1_{L}\epsilon^{3*}_{R}\mathrm{Im}f_1^{(T)} \\ \epsilon^2_{L}\epsilon^{1*}_{R}\mathrm{Im}f_0^{(T)} & \epsilon^2_{L}\epsilon^{2*}_{R}\mathrm{Im}f_0^{(T)} & \epsilon^2_{L}\epsilon^{3*}_{R}\mathrm{Im}f_1^{(T)} \\ \epsilon^3_{L}\epsilon^{1*}_{R}\mathrm{Im}f_1^{(T)} & \epsilon^3_{L}\epsilon^{2*}_{R}\mathrm{Im}f_1^{(T)} & \epsilon^3_{L}\epsilon^{3*}_{R}\mathrm{Im}f_0^{(T)} \end{pmatrix},
\end{aligned}
\tag{4.8}
$$

with

$$
\begin{aligned}
f_1^{(T)} &= \sum_n \frac{(-1)^n}{x+i\pi(n+\nu+\alpha)} \\
&= \begin{cases} \sinh(x+i\pi\alpha)^{-1} & : T=+1(\nu=0) \\ \cosh(x+i\pi\alpha) & : T=-1(\nu=1/2). \end{cases}
\end{aligned}
\tag{4.9}
$$

However, in the case of **15** and **6** rep bulk fermions, the rank of M is two, that is, one massless boundary fermion is remaining. We avoid this problem by introducing two bulk fermions with different bulk masses.

If some bulk and mirror fermions are introduced, all of the contributions for the kinetic and mass mixing in Eq.(4.8) must be summed,

$$
\begin{aligned}
\hat{Z}^{ij}_{L,R} &\equiv \delta^{ij} + \sum_a Z^{a,ij}_{L,R} \\
\hat{M}^{ij} &\equiv \sum_a M^{a,ij}
\end{aligned}
\tag{4.10}
$$

In the expression above, the superscript "a" in $Z^{a,ij}_{L,R}$ and $M^{a,ij}$ mean that its contribution comes from some bulk and mirror fermions.

To obtain the physical masses of the SM fermion, we have to diagonalize the matrices in Eq. (4.10). The kinetic mixing can be diagonalized by unitary matrices $U_{Z_{L,R}}$

$$
\hat{Z}_{L,R} = U^\dagger_{Z_{L,R}} Z^{\mathrm{diag}}_{L,R} U_{Z_{L,R}},
\tag{4.11}
$$

where $Z^{\mathrm{diag}}_{L,R}$ are diagonal matrices. After rewriting the mass term in terms of new basis diagonalizing the kinetic mixings and normalizing the kinetic term, we obtain the following mass matrix

$$
M' = \sqrt{(Z^{\mathrm{diag}}_L)^{-1}}\, U_{Z_L} \hat{M} U^\dagger_{Z_R} \sqrt{(Z^{\mathrm{diag}}_R)^{-1}}.
\tag{4.12}
$$

Next, we perform unitary transformation in order to move on to the mass basis of the SM:

$$
\psi'_R = U_R \psi_R, \qquad \psi'_L = U_L \psi_L.
\tag{4.13}
$$

In this new basis, the physical mass matrix is obtained

$$M^{\rm diag} \equiv U_L M' U_R^\dagger = {\rm diag}(m^1_{\rm phys}, m^2_{\rm phys}, m^3_{\rm phys}), \tag{4.14}$$

where $m^i_{\rm phys}(i = 1, 2, 3)$ are the physical masses of the i-th generation of the SM fermions, the charged lepton and the neutrino, respectively.

We have to take into account the mixing effects between the bulk and the boundary fermions. The additional mixing in the charged weak interaction of the boundary fermion, which is not present in the SM, seems to be generated. According to the interactions between the bulk and the boundary fermions in Eq. (4.5) and the weak interaction of the bulk and mirror fermions

$$-\frac{g}{\sqrt{2}}\sum_n W^+_\mu \overline{\psi^{u(n)}}\gamma^\mu \psi^{d(n)} - \frac{g}{\sqrt{2}}\sum_n W^+_\mu \overline{\tilde{\psi}^{u(n)}}\gamma^\mu \tilde{\psi}^{d(n)}, \tag{4.15}$$

the additional mixing in the charged weak interaction of the boundary fermion is given by

$$-\frac{g}{\sqrt{2}}\sum_{i,j} W^+_\mu \overline{u^i_L}\gamma^\mu M^{ij}_{\rm WI} d^j_L + {\rm h.c}, \tag{4.16}$$

where [2]

$$\begin{aligned}\gamma^\mu M^{ij}_{\rm WI} P_L = P_R \sum_n \frac{\xi^{ij}_n \epsilon^{ui}_L \epsilon^{dj*}_L}{(\pi R)^2} \Big\{ &\left\langle \psi^{u(n)}\overline{\psi^{u(n)}}\right\rangle_E \gamma^\mu \left\langle \psi^{d(n)}\overline{\psi^{d(n)}}\right\rangle_E \\ &+ \left\langle \psi^{u(n)}\overline{\tilde{\psi}^{u(n)}}\right\rangle_E \gamma^\mu \left\langle \psi^{d(n)}\overline{\tilde{\psi}^{d(n)}}\right\rangle_E \Big\}.\end{aligned} \tag{4.17}$$

The KK fields of the bulk fermions interacting to u_L (d_L) and the strength are denoted by $\psi^{u(d)}$ ($\psi^{u(d)}$) and ϵ^u_L (ϵ^d_L), respectively. $\xi^{i,j}_n$ is $(-1)^n$ in the case of $(i, j) = (1, 3), (2, 3), (3, 1), (3, 2)$ or 1 in the other case. Similarly, this contribution can be rewritten by the functions in Eq. (3.9) and Eq. (4.9). Then, we found the additional mixing in the charged weak interaction to be the same as the kinetic mixing for the left-handed fermions localized on the boundary,

$$M^{ij}_{\rm WI} = Z^{ij}_L. \tag{4.18}$$

This property ensure that no additional mixings is needed as will be shown below. In the case where some bulk and mirror fermions are introduced, the kinetic and mass mixing are the summation of all contributions in Eq. (4.17),

$$\hat{M}^{ij}_{\rm WI} = \delta^{ij} + \sum_a M^{ij}_{{\rm WI},a} = \hat{Z}^{ij}_L. \tag{4.19}$$

[2]The subscript "I" in $M_{\rm WI}$ is put to avoid a confusion with the W boson mass.

bulk fermion $SU(6) \to SU(5)$	mirror fermion
$20^{(+,+)} = 10 \oplus 10^*$	$20^{(-,-)}$
$15^{(+,+)} = 10 \oplus 5$	$15^{(-,-)}$
$15'^{(+,-)} = 10' \oplus 5'$	$15'^{(-,+)}$
$6^{(-,-)} = 5 \oplus 1$	$6^{(+,+)}$
$6'^{(+,+)} = 5' \oplus 1'$	$6'^{(-,-)}$

Table 5: Representation of bulk fermions and the corresponding mirror fermions. P_i are parity of bulk fermion for representation $\mathbf{i}$ in $SU(6)$. R in $R^{(+,+)}$ means an $SU(6)$ representation of the bulk fermion. r_i in $r_1 \oplus r_2$ are $SU(5)$ representations.

After rewriting the charged weak interaction in terms of new basis in Eq. (4.13), CKM matrix and PMNS matrix are given by

$$\begin{aligned} V_{\rm CKM} &= U_L^u \sqrt{(Z_L^{{\rm diag},u})^{-1}} U_{Z_L}^u \hat{M}_{\rm WI}^{ud} U_{Z_L}^{d\dagger} \sqrt{(Z_L^{{\rm diag},d})^{-1}} U_L^{d\dagger} \\ &= U_L^u \sqrt{(Z_L^{{\rm diag},u})^{-1}} Z_L^{{\rm diag},u} \sqrt{(Z_L^{{\rm diag},d})^{-1}} U_L^{d\dagger} \\ &= U_L^u U_L^{d\dagger}, \\ V_{\rm PMNS} &= U_L^e \sqrt{(Z_L^{{\rm diag},e})^{-1}} U_{Z_L}^e \hat{M}_{\rm WI}^{e\nu} U_{Z_L}^{\nu\dagger} \sqrt{(Z_L^{{\rm diag},\nu})^{-1}} U_L^{\nu\dagger} \\ &= U_L^e \sqrt{(Z_L^{{\rm diag},e})^{-1}} Z_L^{{\rm diag},\nu} \sqrt{(Z_L^{{\rm diag},\nu})^{-1}} U_L^{\nu\dagger} \\ &= U_L^e U_L^{\nu\dagger}, \end{aligned} \tag{4.20}$$

We utilized the fact that the contributions of the left-handed $SU(2)$ doublets to the kinetic mixing are the same, for instance, $\hat{Z}_L^u = \hat{Z}_L^d$ and $\hat{Z}_L^e = \hat{Z}_L^\nu$.

The expressions in Eq. (4.14) and (4.20) allow us to calculate the SM fermion masses and the flavor mixing angles, respectively. The quarks and leptons are introduced at $y = 0$ and $y = \pi R$ boundary,

$$\begin{aligned} \mathcal{L}_{\rm SM}^{j=1,2} &= \delta(y)[\bar{\chi}_{10}^j i\Gamma^\mu D_\mu \chi_{10}^j + \bar{\chi}_{5^*}^j i\Gamma^\mu D_\mu \chi_{5^*}^j + \bar{\chi}_1^j i\Gamma^\mu D_\mu \chi_1^j], \\ \mathcal{L}_{\rm SM}^{j=3} &= \delta(y-\pi R)[\bar{q}_L^3 i\Gamma^\mu D_\mu q_L^3 + \bar{u}_R^3 i\Gamma^\mu D_\mu u_R^3 + \bar{d}_R^3 i\Gamma^\mu D_\mu d_R^3 \\ &\quad + \bar{l}_L^3 i\Gamma^\mu D_\mu l_L^3 + \bar{e}_R^3 i\Gamma^\mu D_\mu e_R^3 + \bar{\nu}_R^3 i\Gamma^\mu D_\mu \nu_R^3]. \end{aligned} \tag{4.21}$$

since the gauge symmetry $SU(5)$ remains at $y = 0$, the quarks and leptons are embedded into $SU(5)$ multiplets, χ_{10}, χ_{5^*} and χ_1. On the other hand, the quark and lepton localized at $y = \pi R$ are embedded into SM multiplets because the gauge symmetries $SU(3)_C \times SU(2)_L \times U(1)_Y$ are unbroken at $y = \pi R$. We introduce one **20** rep bulk fermion, two **15** rep bulk fermions and two **6** rep fermions and the corresponding mirror fermions shown in Table 5. The interactions of these bulk fermions with the boundary fermions are given

bulk fermion $SU(5) \to SU(3)_C \times SU(2)_L \times U(1)_Y$	SM fermion coupling to bulk
$10 = Q_{20}(3,2)^{(+,+)}_{1/6} \oplus U^*_{20}(3^*,1)^{(+,-)}_{-2/3} \oplus E^*_{20}(1,1)^{(+,-)}_{1}$	$q_L(3,2)_{1/6},\ u^c_R(3^*,1)_{-2/3},\ e^c_R(1,1)_1$
$10^* = Q^*_{20}(3^*,2)^{(-,-)}_{-1/6} \oplus U_{20}(3,1)^{(-,+)}_{2/3} \oplus E_{20}(1,1)^{(-,+)}_{-1}$	$q^c_L(3^*,2)_{-1/6},\ u_R(3,1)_{2/3},\ e_R(1,1)_{-1}$

Table 6: **20** bulk fermion and SM fermions. $r_{1,2}$ in $(r_1,\ r_2)_a$ are $SU(3),\ SU(2)$ representations in the SM, respectively. a is $U(1)_Y$ charges.

bulk fermion $SU(5) \to SU(3)_C \times SU(2)_L \times U(1)_Y$	SM fermion coupling to bulk
$10 = Q_{15}(3,2)^{(+,-)}_{1/6} \oplus U^*_{15}(3^*,1)^{(+,+)}_{-2/3} \oplus E^*_{15}(1,1)^{(+,+)}_{1}$	$q_L(3,2)_{1/6},\ u^c_R(3^*,1)_{-2/3},\ e^c_R(1,1)_1$
$5 = D_{15}(3,1)^{(-,+)}_{-1/3} \oplus L^*_{15}(1,2)^{(-,-)}_{1/2}$	$d_R(3,1)_{-1/3},\ l^c_L(1,2)_{1/2}$
bulk fermion $SU(5) \to SU(3)_C \times SU(2)_L \times U(1)_Y$	SM fermion coupling to bulk
$10' = Q_{15'}(3,2)^{(+,+)}_{1/6} \oplus U^*_{15'}(3^*,1)^{(+,-)}_{-2/3} \oplus E^*_{15'}(1,1)^{(+,-)}_{1}$	$q_L(3,2)_{1/6},\ u^c_R(3^*,1)_{-2/3},\ e^c_R(1,1)_1$
$5' = D_{15'}(3,1)^{(-,-)}_{-1/3} \oplus L^*_{15'}(1,2)^{(-,+)}_{1/2}$	$d_R(3,1)_{-1/3},\ l^c_L(1,2)_{1/2}$

Table 7: Upper (Lower) table shows **15** (**15**$'$) bulk fermion and SM fermions. $r_{1,2}$ in $(r_1,\ r_2)_a$ are $SU(3),\ SU(2)$ representations in the SM, respectively. a is $U(1)_Y$ charges.

bulk fermion $SU(5) \to SU(3)_C \times SU(2)_L \times U(1)_Y$	SM fermion coupling to bulk
$5 = D_6(3,1)^{(-,+)}_{-1/3} \oplus L^*_6(1,2)^{(-,-)}_{1/2}$	$d_R(3,1)_{-1/3},\ l^c_L(1,2)_{1/2}$
$1 = N^*_6(1,1)^{(+,+)}_{0}$	$\nu^c_R(1,1)_0$
bulk fermion $SU(5) \to SU(3)_C \times SU(2)_L \times U(1)_Y$	SM fermion coupling to bulk
$5' = D_{6'}(3,1)^{(+,-)}_{-1/3} \oplus L^*_{6'}(1,2)^{(+,+)}_{1/2}$	$d_R(3,1)_{-1/3},\ l^c_L(1,2)_{1/2}$
$1' = N^*_{6'}(1,1)^{(-,-)}_{0}$	$\nu^c_R(1,1)_0$

Table 8: Upper (Lower) table shows **6** (**6**$'$) bulk fermion and SM fermions. $r_{1,2}$ in $(r_1,\ r_2)_a$ are $SU(3),\ SU(2)$ representations in the SM, respectively. a is $U(1)_Y$ charges.

by

$$\begin{aligned}\mathcal{L}^{j=1,2}_{\rm SM+bulk} &= \delta(y)\sqrt{\frac{2}{\pi R}}[\epsilon^j_{20}(\bar\chi^j_{10}\Psi_{10\subset 20} + \bar\chi^{j,c}_{10}\Psi_{10^*\subset 20}) \\ &+\epsilon^j_{15}(\bar\chi^j_{10}\Psi_{10\subset 15} + \bar\chi^{j,c}_{5^*}\Psi_{5\subset 15}) + \epsilon^j_{15'}(\bar\chi^j_{10}\Psi_{10'\subset 15'} + \bar\chi^{j,c}_{5^*}\Psi_{5'\subset 15'}) \\ &+\epsilon^j_{6}(\bar\chi^{j,c}_{5^*}\Psi_{5\subset 6} + \bar\chi^j_{1}\Psi_{1\subset 6}) + \epsilon^j_{6'}(\bar\chi^{j,c}_{5^*}\Psi_{5'\subset 6'} + \bar\chi^j_{1}\Psi_{1'\subset 6'}) + \text{h.c.}], \quad (4.22)\end{aligned}$$

$$\begin{aligned}\mathcal{L}^{j=3}_{\rm SM+bulk} &= \delta(y-\pi R)\sqrt{\frac{2}{\pi R}}[\epsilon_{20e}(\bar e^3_R E_{20} + \bar u^3_R U_{20}) + \epsilon_{20q}\bar q^3_L Q_{20} \\ &+\epsilon_{15u}\bar u^{3,c}_R U^*_{15} + \epsilon_{15e}(\bar e^{3,c}_R E^*_{15} + \bar l^{3,c}_L L^*_{15}) + \epsilon_{15'd}(\bar q^3_L Q_{15'} + \bar d^3_R D_{15'}) \\ &+\epsilon_{6\nu}(\bar l^{3,c}_L L^*_6 + \bar\nu^{3,c}_R N^*_6) + \epsilon_{6'd}\bar d^3_R D_{6'} + \text{h.c.}]. \quad (4.23)\end{aligned}$$

ϵ are the strength of the mixing term between the bulk fermion and the SM fermions and should be complex numbers so that we can avoid a problem of vanishing the determinant of mass matrix. The decomposition of the introduced bulk fermions in the **20**, **15** (**15**'),

$1/R$	c	m_u	m_c	m_t	
10TeV	80	2.163 MeV	1.217 GeV	166.294 GeV	
10TeV	90	2.320 MeV	1.229 GeV	167.931 GeV	
15TeV	80	2.316 MeV	1.214 GeV	165.300 GeV	
15TeV	90	2.156 MeV	1.225 GeV	166.89 GeV	
Data		$2.16^{+0.49}_{-0.26}$ MeV	1.27 ± 0.02 GeV	172 ± 0.30 GeV	
$1/R$	c	m_d	m_s	m_b	
10TeV	80	5.583 MeV	75.7 MeV	4.155 GeV	
10TeV	90	5.505 MeV	75.8 MeV	4.321 GeV	
15TeV	80	5.522 MeV	75.5 MeV	4.201 GeV	
15TeV	90	5.545 MeV	75.1 MeV	4.183 GeV	
Data		$4.67^{+0.48}_{-0.17}$ MeV	93^{+11}_{-5} MeV	$4.18^{+0.13}_{-0.02}$ GeV	
$1/R$	c	$\sin\theta_{12}$	$\sin\theta_{13}$	$\sin\theta_{23}$	δ
10TeV	80	0.191797	0.003537	0.041430	1.1560
10TeV	90	0.195857	0.003510	0.039893	1.2424
15TeV	80	0.190839	0.003556	0.041459	1.1831
15TeV	90	0.192085	0.003518	0.040088	1.1750
Data		0.22650 ± 0.00048	$0.00361^{+0.00011}_{-0.00009}$	$0.04053^{+0.00083}_{-0.00061}$	$1.196^{+0.045}_{-0.043}$

Table 9: Our results of parameter fitting in quark sector for some parameters $1/R$ and $c = c_1 + c_2$. The up, down, and strange quark masses are the $\overline{\rm MS}$ masses at the scale $\mu =$ 2 GeV. The charm and bottom quark masses are the $\overline{\rm MS}$ masses renormalized at the $\overline{\rm MS}$ mass, i.e. $\bar{m} = \bar{m}(\mu = \bar{m})$. The top quark mass is extracted from direct measurements.

6 (**6**') representations into the SM gauge group and the corresponding the SM fermions to be coupled on the boundary are summarized in Tables 6, 7, 8, respectively. Note that only the (conjugate of) bulk fermions with parities $(+,+)$ $((-,-))$ can couple to the SM fermions on the boundary.

Finally, we analyze the SM fermion masses and the flavor mixing angles numerically, and have found the suitable parameter sets reproducing these experimental values. Some sample data sets are shown in Table 9 and 10. In this analysis, we refer to the experimental data of CKM and PMNS matrices shown in Particle Data Group [14]. As for the neutrino hierarchy, we assume the normal hierarchy although it is not essential. The results are remarkable since the generation mixing in the bulk and newly introduced resulting from the reduction of the number of bulk fermions, which makes, in particular, reproducing the quark and lepton mixing angles highly nontrivial.

$1/R$	c	m_e	m_μ	m_τ
10TeV	80	0.5136 MeV	98.750 MeV	1687.12 MeV
10TeV	90	0.5140 MeV	98.188 MeV	1689.56 MeV
15TeV	80	0.5135 MeV	98.776 MeV	1695.46 MeV
15TeV	90	0.5139 MeV	98.610 MeV	1687.59 MeV
Data		0.5109989461(31) MeV	105.6583745(24) MeV	1776.86(12) MeV
$1/R$	c	Δm^2_{21}	Δm^2_{32} (Normal)	δ
10TeV	80	$7.7306 \times 10^{-5}\,\mathrm{eV}^2$	$2.4524 \times 10^{-3}\,\mathrm{eV}^2$	1.539π rad
10TeV	90	$7.7087 \times 10^{-5}\,\mathrm{eV}^2$	$2.4367 \times 10^{-3}\,\mathrm{eV}^2$	1.536π rad
15TeV	80	$7.8054 \times 10^{-5}\,\mathrm{eV}^2$	$2.3895 \times 10^{-3}\,\mathrm{eV}^2$	1.531π rad
15TeV	90	$7.6544 \times 10^{-5}\,\mathrm{eV}^2$	$2.4577 \times 10^{-3}\,\mathrm{eV}^2$	1.536π rad
Data		$(7.53 \pm 0.18) \times 10^{-5}\,\mathrm{eV}^2$	$(2.453 \pm 0.033) \times 10^{-3}\,\mathrm{eV}^2$	$1.36^{+0.20}_{-0.16}\pi$ rad
$1/R$	c	$\sin^2\theta_{12}$	$\sin^2\theta_{13}$	$\sin^2\theta_{23}$ (Normal)
10TeV	80	0.3313	2.240×10^{-2}	0.5161
10TeV	90	0.3294	2.155×10^{-2}	0.5187
15TeV	80	0.3505	2.094×10^{-2}	0.5069
15TeV	90	0.3308	2.123×10^{-2}	0.5161
Data		0.307 ± 0.013	$(2.20 \pm 0.07) \times 10^{-2}$	0.546 ± 0.021

Table 10: Our results of parameter fitting in lepton sector for some parameters $1/R$ and $c = c_1 + c_2$. In neutrino sector, the normal hierarchy is assumed.

5 Gauge Coupling unification in gGHU

In $SU(6)$ grand Gauge-Higgs unification, Standard Model gauge symmetry $SU(3)_C \times SU(2)_L \times U(1)_Y$ should be unified to $SU(6)$ in higher dimension. Therefore, in this section we discuss the gauge coupling running for the SM gauge symmetry. In the first half of this section, we explain how the gauge couplings run with the contribution of KK fields. In the second half of this section, we analyze the gauge coupling running of the models introduced in Sec. 3 and Sec. 4. In the latter model, the perturbative gauge couplings are realized.

5.1 Gauge coupling running in the Standard Model

In four-dimensional case, the energy dependence of the gauge couplings are determined by the renormalization group equation (RGE),

$$\frac{d}{d\ln\mu}\alpha_i^{-1}(\mu) = -\frac{b_i}{2\pi}, \tag{5.1}$$

where μ is a renormalization scale, $\alpha_i = g_i^2/4\pi$, and $i = Y, 2, 3$ denotes the SM gauge group $U(1)_Y$, $SU(2)_L$ and $SU(3)_C$, respectively. b_i is the one-loop beta function coefficient, which is given by

$$b_i = \begin{cases} -11/3 \times T(R_V) & : \text{Gauge field} \\ 2/3 \times T(R_F) & : \text{Weyl fermion} \\ 2/6 \times T(R_S) & : \text{Scalar field} \end{cases}, \tag{5.2}$$

where R_i denotes the representation of the fields. $T(R_V)$ is the quadratic Casimir invariant of the adjoint representation T_V and $T(R_{F,S})$ are the Dynkin indices of the irreducible representation $R_{F,S}$. In the SM, the beta functions are obtained as

$$(b_Y, b_2, b_3) = \left(\frac{41}{6}, -\frac{19}{6}, -7\right). \tag{5.3}$$

The solutions of RGE in Eq. (5.1) are given by

$$\alpha_i^{-1}(\Lambda) = \alpha_i^{-1}(\mu) - \frac{b_i}{2\pi}\ln\frac{\Lambda}{\mu}, \tag{5.4}$$

where Λ is the cutoff scale of the theory. Thus, the SM gauge couplings depend on the energy scale logarithmically.

In $SU(5)$ GUT, the gauge couplings satisfy the following relation at the unification scale Λ_G,

$$\alpha_G^{-1} = \frac{3}{5}\alpha_Y^{-1}(\Lambda_G) = \alpha_2^{-1}(\Lambda_G) = \alpha_3^{-1}(\Lambda_G), \tag{5.5}$$

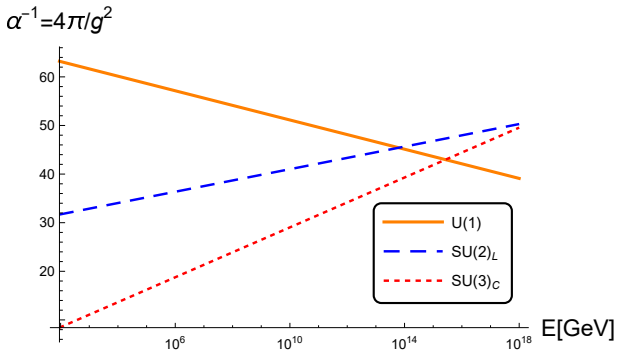

Figure 9: The energy dependence of the SM gauge couplings, which is defined by Eq. (5.4) and Eq. (5.6).

where α_G is the gauge coupling constant at the unification scale. The factor of the $3/5$ comes from the different normalization of the generators between $U(1)_Y$ group and $U(1)$ group under the $SU(5)$ group, $T_Y = \sqrt{5/3}T_{U(1)\subset SU(5)}$. Then, we can relate the gauge coupling α_Y to $\alpha_1 = 5/3\alpha_Y$ and from Eq. (5.1) the beta functions are also rewritten as

$$(b_1, b_2, b_3) = \left(\frac{41}{10}, -\frac{19}{6}, -7\right). \tag{5.6}$$

Fig. 9 shows the gauge coupling running in the SM. We have taken the Z boson mass to be $M_Z \sim 91.17$ GeV as a low-energy reference scale. Fig. 9 indicates that the gauge coupling unification in SM cannot be realized at one-loop level. Therefore, the extension of the SM is necessary to explore the feasibility of the gauge coupling unification.

5.2 Gauge coupling running in the extra-dimensional model

To obtain the energy dependence of the gauge coupling constant in higher dimensional theory we consider the vacuum polarization [12], which is given by

$$\alpha_i^{-1}(\Lambda) = (1 - \Pi_i(0))\,\alpha_i^{-1}(\mu). \tag{5.7}$$

$\Pi_i(0)$ is the vacuum polarization with zero momentum at one-loop level and given by

$$\Pi_i(0) = b_i \frac{g_i^2}{16\pi^2} \int_{\frac{\pi}{4}\Lambda^{-2}}^{\frac{\pi}{4}\mu^{-2}} \frac{dt}{t} \mathcal{P}(t), \tag{5.8}$$

with

$$\mathcal{P}(t) = \sum_n \exp\{-tm_n^2\}, \tag{5.9}$$

where n denotes KK index of the fields propagating in the loop. For instance, when only one particle propagates in the loop, $\Pi_i(0)$ can be calculated as

$$\Pi_i(0) = b_i \frac{g_i^2}{16\pi^2} \int_{\frac{\pi}{4}\Lambda^{-2}}^{\frac{\pi}{4}\mu^{-2}} \frac{dt}{t} \exp\{-tm^2\} = b_i \frac{g_i^2}{8\pi^2} \ln\frac{\Lambda}{\mu}, \tag{5.10}$$

which lead to

$$\alpha_i^{-1}(\Lambda) = (1 - \Pi_i(0))\,\alpha_i^{-1}(\mu) = \alpha_i^{-1}(\mu) - \frac{b_i}{2\pi}\ln\frac{\Lambda}{\mu} \tag{5.11}$$

This is the usual logarithmic running of the gauge coupling in SM shown in Eq. (5.4).

In the case of KK-fields with mass $m_n^2 = (n+\nu+\alpha)^2/R^2 + (\lambda/\pi R)^2$, the integrand is given by

$$\mathcal{P}(t) = \theta_{3-2\nu}\left(i\alpha t/R^2, \exp[-t/R^2]\right)\exp\left[-\frac{t}{R^2}(\alpha^2+\lambda^2)\right], \tag{5.12}$$

where θ_i $(i = 2, 3)$ are the elliptic theta functions

$$\begin{aligned}\theta_2(v,q) =& 2q^4\sum_{n=0}^{\infty} q^{n(n+1)}\cos[(2n+1)v],\\ \theta_3(v,q) =& 1 + 2\sum_{n=1}^{\infty} q^{n^2}\cos[2nv].\end{aligned} \tag{5.13}$$

They exhibit different behaviors from the logarithmic one in the SM. When the energy scale Λ and μ are sufficiently larger than the compactification scale, the elliptic theta function can be approximated as follows,

$$\theta_i \sim R\sqrt{\frac{\pi}{t}}, \tag{5.14}$$

and we obtain

$$\begin{aligned}\Pi(0) \sim& \frac{g^2}{16\pi^2}\int_{\frac{\pi}{4}\Lambda^{-2}}^{\frac{\pi}{4}\mu^{-2}}\frac{dt}{t}R\sqrt{\frac{\pi}{t}}\\ =& \frac{g^2}{8\pi^2}\left[2\left\{(R\Lambda)e^{-\frac{\pi\lambda^2}{4(R\Lambda^2)}} - (R\mu)e^{-\frac{\pi\lambda^2}{4(R\mu^2)}}\right\} + \lambda\pi\mathrm{Erf}\left[\frac{\sqrt{\pi}}{2}\frac{\lambda}{R\mu}, \frac{\sqrt{\pi}}{2}\frac{\lambda}{R\Lambda}\right]\right]\\ \sim& \frac{g^2}{4\pi^2}R(\Lambda-\mu),\end{aligned} \tag{5.15}$$

where Erf is the error function, $\mathrm{Erf}[a,b] = \frac{1}{\sqrt{\pi}}\int_b^a dte^{-t^2}$. Eq. (5.15) shows the contribution from KK field to the vacuum polarization depends linearly on the energy scale, not logarithmically.

From Eq. (5.7), the running of the gauge coupling is derived as

$$\alpha_i^{-1}(\lambda) = \alpha_i^{-1}(\mu) - \frac{b_i - \tilde{b}_i^{(+)}}{4\pi}\ln\frac{\Lambda}{\mu} - \frac{\tilde{b}_i^{(+)} + \tilde{b}_i^{(-)}}{\pi}R(\Lambda-\mu). \tag{5.16}$$

Here $\tilde{b}^{(+)}(\tilde{b}^{(-)})$ denotes the beta function for (anti-)periodic field and b stands for the beta function for the boundary fermion.

If the beta functions of the KK field satisfies the relation

$$\tilde{b}_i^{(+)} + \tilde{b}_i^{(-)} < 0, \tag{5.17}$$

our theory is asymptotically free, because the power running effects overcome those of logarithmic running at high energy.

5.3 Analysis of the gauge coupling unification

We analyze the gauge coupling running in two cases discussed in Sec. 3 and Sec. 4. In the former case, the fields in the bulk are the **35** representation gauge field and the three sets of the **20**, **15**, **6** rep bulk and mirror fermions. **35**, **6**, **15** and **20** representations have the value of T in Eq. (5.2) are 6, 1/2, 2 and 3, respectively. Noting that there are the same number of the bulk and the mirror fermions and they contribute to the beta functions of KK fields as Dirac fermions, the beta function of KK fields are given by $\tilde{b}_i^{(+)} + \tilde{b}_i^{(-)} = (-11/3) \times 6 + (4/3) \times (11/2) \times 2 \times 3 = 22 > 0$. Therefore, asymptotic freedom are not achieved.

In the latter case, the fields in the bulk are the **35** representation gauge field and one **20** and two sets of **15** and **6** rep bulk and mirror fermions, thus the beta function of KK fields are given by

$$\tilde{b}_i^{(+)} + \tilde{b}_i^{(-)} = -\frac{11}{3} \times 6 + \frac{4}{3} \times \left(\frac{1}{2} \times 2 + 2 \times 2 + 3 \right) \times 2 = -\frac{2}{3} < 0. \tag{5.18}$$

Therefore, this model is asymptotically free. Fig. 10 shows the energy dependence of the gauge couplings and the difference of each pair of the gauge couplings at $c = c_1 + c_2 = 80$, $r = c_1/(c_1 + c_2) = 0$ and $R^{-1} = 10$ TeV. Since the differences of the gauge coupling $\alpha_i^{-1} - \alpha_j^{-1}$ $(i, j = 1, 2, 3)$ in this figure cannot be equal to 0 at the same energy scale, the unification scale M_G and the unification coupling α_G (g_G) are identified with the energy scale where $U(1)$ and $SU(2)_L$ couplings are unified. We obtain $M_G \sim 2.1 \times 10^{14}$ GeV and $\alpha_G^{-1} \sim 4.4 \times 10^9$ $(g_G \sim 5.3 \times 10^{-5})$. The difference between the unification coupling and $SU(3)_C$ coupling at the unification scale is found as $\left|(\alpha_G^{-1} - \alpha_3^{-1})/\alpha_G^{-1}\right| \sim 5 \times 10^{-10}$ $(|(g_G - g_3)/g_G| \sim 2.6 \times 10^{-10})$, therefore three gauge couplings unify with an accuracy of 10^{-10}. Alternatively, assuming the unification of three couplings α_G at M_G, and evolving $SU(3)_C$ coupling down to the weak scale by Eq. (5.16), $\alpha_3^{-1}(M_z) \sim 10.7$ $(g_3 \sim 1.08)$ is found, which is lager (smaller) than the experimental value $\alpha_3^{-1} \sim 8.3$ $(g_3 \sim 1.2)$. We also analyze $r = 1/2$ and $r = 1$ cases. In the former case, almost the same result as $r = 0$ case is obtained. In the latter case, the differences are smaller $(\sim 10^{-11})$, the unification scale is larger $(M_G \sim 4.1 \times 10^{15})$ and $SU(3)_C$ couplings at the weak scale is lager $(\alpha_3 \sim 13.2)$. We analyze the coupling unification in other parameter cases, (c, r, R^{-1}) =(80,0,15 TeV), (90,0,10 TeV), (90,0,15 TeV) shown in Table 9 and 10 and the

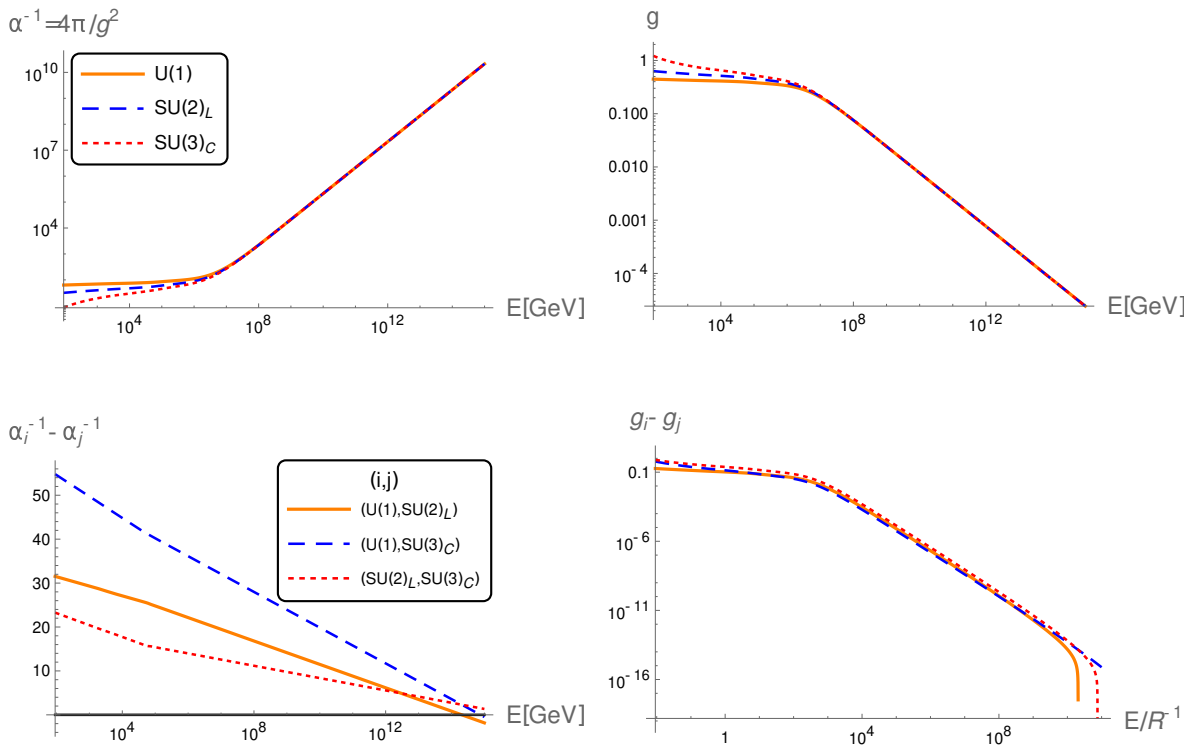

Figure 10: The perturbative gauge coupling unification in the case of $c = 80$, $r = 0$ and $R^{-1} = 10$ TeV. The upper figures shows the energy dependence of gauge coupling α^{-1} (left) and g (right). The lower figures shows the energy dependence of deference between each of the gauge couplings $\alpha_i^{-1} - \alpha_j^{-1}$ (left) and $g_i - g_j$ (right).

results are shown in Table 11. The unification scale in our model is comparable to that of four-dimensional GUT, since the running of coupling constant in $t/R^2 \gg 1$ region is dominated by the contributions linearly dependent on the energy scale and beta functions in Eq. (5.18) are common, then the differences of each pair of the gauge couplings are dominated by the logarithmic terms. In each case shown in Table 11, the theoretical value for $SU(3)_C$ coupling with one-loop corrections at weak scale are slightly deviated from the experimental value. We can analyze two-loop corrections to obtain more accurate unification since the difference of the each pair of the couplings at M_G is extremely small.

We further analyze the coupling unification in the case of larger compactification scale, which was not analyzed in section 4. Although this case is not realistic since the Higgs mass is likely to be enhanced, the SM fermion masses and mixings can be reproduced in lager compactification scale. The results are shown in Table 12. In the range of $R^{-1} = 200$ TeV $-$ 220 TeV, $SU(3)$ coupling at the weak scale can be within a range of error of experimental value.

c	r	R^{-1}	M_G	α_G^{-1}	$\left\|(\alpha_G^{-1} - \alpha_3^{-1})/\alpha_G^{-1}\right\|$	$\alpha_3^{-1}(M_Z)$
80	0	10 TeV	2.1×10^{14} GeV	4.4×10^{9}	5.26×10^{-10}	10.7
80	0	15 TeV	2.2×10^{14} GeV	3.2×10^{10}	6.12×10^{-10}	10.4
90	0	10 TeV	2.1×10^{14} GeV	4.3×10^{9}	5.25×10^{-10}	10.7
90	0	15 TeV	2.3×10^{14} GeV	3.2×10^{9}	6.1×10^{-10}	10.4

Table 11: The results of gauge coupling unification analysis at $r = 0$. The unification scale M_G and the unification coupling α_G^{-1} are identified with the case when $U(1)$ and $SU(2)_L$ couplings unify. $\left|(\alpha_G^{-1} - \alpha_3^{-1})/\alpha_G^{-1}\right|$ is the difference between α_G^{-1} and $SU(3)_C$ coupling at M_G. $\alpha_3^{-1}(M_Z)$ is the $SU(3)$ coupling at the weak scale, assuming that three gauge couplings unify to α_G^{-1} at M_G.

c	r	R^{-1}	M_G	α_G^{-1}	$\alpha_3^{-1}(M_Z)$
80	0	200 TeV	3.8×10^{14} GeV	4.1×10^{8}	8.55
80	0	220 TeV	4.0×10^{14} GeV	3.8×10^{8}	8.49

Table 12: The results of gauge coupling unification analysis in the case of large compactified scale at $r = 0$. The unification scale M_G and the unification coupling α_G^{-1} are identified with the case when $U(1)$ and $SU(2)_L$ couplings unify. $\alpha_3^{-1}(M_Z)$ is the $SU(3)$ coupling at the weak scale, assuming that three gauge couplings unify to α_G^{-1} at M_G.

6 Conclusions

In this thesis, we have first discussed the fermion mass hierarchy in $SU(6)$ gGHU. The SM fermions are introduced on the $y = 0$ boundary as $SU(5)$ multiplets. We also introduced three sets of the **20**, **15** and **6** rep bulk and mirror fermions. Integrating out these fermions, we obtain the SM fermion masses except for top quark. To achieve the enhancement of masses, we introduced the localized gauge kinetic terms on the boundaries. By analyzing the masses with these terms, the parities of the bulk fermions and suitable parameter region were found.

Second, we have discussed the flavor mixing angles in $SU(6)$ gGHU. Since the previous model [1] has no flavor mixing term, we modified the interactions between the bulk and SM fermions to obtain the flavor mixings. Thanks to this modification, the number of the bulk fermions required to reproduce the SM fermion masses is reduced and the interactions between the SM and bulk fermions become intergenerational. We have shown that the fermion mass hierarchy and the flavor mixing angles can be reproduced by mild turning the free parameters.

Finally, we have discussed the gauge coupling unification in $SU(6)$ gGHU. Since the energy dependence of the gauge couplings in five-dimensional theory is not logarithmically running but linearly, the asymptotic freedom of the theory is nontrivial and have to be checked. We computed the beta functions in two previous model [2] and [3] and found that latter model is asymptotic free. This fact is due to the reduction of the number of the bulk and mirror fermions by introducing the flavor mixing terms. Although the unification scale in the higher-dimensional theory is expected to be very small compared to the four-dimensional GUT scale 10^{15-16} GeV, we found the unification scale $\sim 10^{14}$ GeV which is a few order smaller than the four-dimensional GUT scale. This is because the energy dependence of the difference between each pair of the gauge couplings is not linearly but logarithmically since three beta functions of the KK fields, which is the coefficient of the linearly running term, are common. This is because all KK-fields are embedded into multiplets of the unified gauge group, which is an $SU(6)$ group in our model.

Through the above three topics, we construct the base of the realistic gGHU model. However, there is an issue to be explored in a context of GUT scenario, specifically, a proton decay. The X and Y gauge boson masses in the large extra dimensional model such as gGHU are likely to be comparable to compactification scale. Thus, the proton decay will occur very rapidly in this model. Here, we propose two ideas to avoid this problem.

Since X and Y gauge bosons in our model do not present on the $y = \pi R$ boundary but on the $y = 0$ boundary, if the first generation of the SM fermions are embedded in the $y = \pi R$ boundary and the strengths of the their interaction of X, Y gauge bosons generating the flavor mixing are very small, a proton decay rate obtains suppression factors. The other idea is imposing some symmetry in our model and forbidding the possible dangerous baryon violating operators (see [15] for UED case). It would be also interesting to investigate the main decay mode of the proton decay in our model and give predictions for Hyper Kamiokande experiments.

Acknowledgments

First of all, I express my sincere thanks to Prof. Nobuhito Maru for supporting my Ph.D course and invaluable advice regarding my research. I am grateful to Masato Yamanaka, Haruki Takahashi and Issei Osako for helpful discussion as my collaborator. During my Ph.D course, I am supported by the member of Particle Physics Group, Mathematical Physics Group and Theoretical Astrophysics Group in Osaka Metropolitan University. In particular, I receive helpful guidance from Prof. Nobuhito Maru, Prof. Hiroshi Itoyama, Prof. Hideki Ishihara and Prof. Ken-ich Nakao about the quantum field theory, relativity and cosmology and I am grateful to them. I also would like to thanks Satsuki Mastuno, Kazuki Kiyoshige, Nobuyuki Asaka, Kazumasa Okabayashi, Sota Nakazima, Tomohiro Furukawa, katsuya Yano Akira Okawa, Ryota Endo, Suzuki Mitsuyo and Takuya Hirose for fruitful discussion.

Finally, I would like to thanks my family for their supports in my life. Without their supports I wouldn't have been able to accomplish my study until the end.

This work was supported by JST SPRING, Grant Number JPMJSP2139 (YY).

A The generators of $SU(6)$ group

The generators of $SU(6)$ group $T^a (a = 1 \sim 35)$ are chosen to satisfy the relation,

$$\mathrm{tr}\left[T^a, T^b\right] = 2\delta^{a,b} \tag{A.1}$$

These are shown as bellow.

$$T^1 = \frac{1}{2}\left(\begin{array}{cc|cccc} 0 & 1 & 0 & 0 & 0 & 0 \\ 1 & 0 & 0 & 0 & 0 & 0 \\ \hline 0 & 0 & 0 & 0 & 0 & 0 \\ 0 & 0 & 0 & 0 & 0 & 0 \\ 0 & 0 & 0 & 0 & 0 & 0 \\ \hline 0 & 0 & 0 & 0 & 0 & 0 \end{array}\right), \quad T^2 = \frac{1}{2}\left(\begin{array}{cc|cccc} 0 & -i & 0 & 0 & 0 & 0 \\ i & 0 & 0 & 0 & 0 & 0 \\ \hline 0 & 0 & 0 & 0 & 0 & 0 \\ 0 & 0 & 0 & 0 & 0 & 0 \\ 0 & 0 & 0 & 0 & 0 & 0 \\ \hline 0 & 0 & 0 & 0 & 0 & 0 \end{array}\right),$$

$$T^3 = \frac{1}{2}\left(\begin{array}{cc|cccc} 1 & 0 & 0 & 0 & 0 & 0 \\ 0 & -1 & 0 & 0 & 0 & 0 \\ \hline 0 & 0 & 0 & 0 & 0 & 0 \\ 0 & 0 & 0 & 0 & 0 & 0 \\ 0 & 0 & 0 & 0 & 0 & 0 \\ \hline 0 & 0 & 0 & 0 & 0 & 0 \end{array}\right), \tag{A.2}$$

$$T^4 = \frac{1}{2}\left(\begin{array}{cc|cccc} 0 & 0 & 1 & 0 & 0 & 0 \\ 0 & 0 & 0 & 0 & 0 & 0 \\ \hline 1 & 0 & 0 & 0 & 0 & 0 \\ 0 & 0 & 0 & 0 & 0 & 0 \\ 0 & 0 & 0 & 0 & 0 & 0 \\ \hline 0 & 0 & 0 & 0 & 0 & 0 \end{array}\right), \quad T^5 = \frac{1}{2}\left(\begin{array}{cc|cccc} 0 & 0 & -i & 0 & 0 & 0 \\ 0 & 0 & 0 & 0 & 0 & 0 \\ \hline i & 0 & 0 & 0 & 0 & 0 \\ 0 & 0 & 0 & 0 & 0 & 0 \\ 0 & 0 & 0 & 0 & 0 & 0 \\ \hline 0 & 0 & 0 & 0 & 0 & 0 \end{array}\right),$$

$$T^6 = \frac{1}{2}\left(\begin{array}{cc|cccc} 0 & 0 & 0 & 0 & 0 & 0 \\ 0 & 0 & 1 & 0 & 0 & 0 \\ \hline 0 & 1 & 0 & 0 & 0 & 0 \\ 0 & 0 & 0 & 0 & 0 & 0 \\ 0 & 0 & 0 & 0 & 0 & 0 \\ \hline 0 & 0 & 0 & 0 & 0 & 0 \end{array}\right), \quad T^7 = \frac{1}{2}\left(\begin{array}{cc|cccc} 0 & 0 & 0 & 0 & 0 & 0 \\ 0 & 0 & -i & 0 & 0 & 0 \\ \hline 0 & i & 0 & 0 & 0 & 0 \\ 0 & 0 & 0 & 0 & 0 & 0 \\ 0 & 0 & 0 & 0 & 0 & 0 \\ \hline 0 & 0 & 0 & 0 & 0 & 0 \end{array}\right), \tag{A.3}$$

$$T^8 = \frac{1}{2}\left(\begin{array}{cc|cccc} 0 & 0 & 0 & 0 & 0 & 0 \\ 0 & 0 & 0 & 0 & 0 & 0 \\ \hline 0 & 0 & 1 & 0 & 0 & 0 \\ 0 & 0 & 0 & -1 & 0 & 0 \\ 0 & 0 & 0 & 0 & 0 & 0 \\ \hline 0 & 0 & 0 & 0 & 0 & 0 \end{array}\right),$$

$$
T^9 = \frac{1}{2}\left(\begin{array}{cc|ccc|c} 0&0&0&1&0&0\\ 0&0&0&0&0&0\\ \hline 0&0&0&0&0&0\\ 1&0&0&0&0&0\\ 0&0&0&0&0&0\\ \hline 0&0&0&0&0&0 \end{array}\right),\ T^{10} = \frac{1}{2}\left(\begin{array}{cc|ccc|c} 0&0&0&-i&0&0\\ 0&0&0&0&0&0\\ \hline 0&0&0&0&0&0\\ 0&0&0&0&0&0\\ 0&0&0&0&0&0\\ \hline 0&0&0&0&0&0 \end{array}\right),
$$

$$
T^{11} = \frac{1}{2}\left(\begin{array}{cc|ccc|c} 0&0&0&0&0&0\\ 0&0&0&1&0&0\\ \hline 0&0&0&0&0&0\\ 0&1&0&0&0&0\\ 0&0&0&0&0&0\\ \hline 0&0&0&0&0&0 \end{array}\right),\ T^{12} = \frac{1}{2}\left(\begin{array}{cc|ccc|c} 0&0&0&0&0&0\\ 0&0&0&-i&0&0\\ \hline 0&0&0&0&0&0\\ 0&i&0&0&0&0\\ 0&0&0&0&0&0\\ \hline 0&0&0&0&0&0 \end{array}\right),
$$

$$
T^{13} = \frac{1}{2}\left(\begin{array}{cc|ccc|c} 0&0&0&0&0&0\\ 0&0&0&0&0&0\\ \hline 0&0&0&1&0&0\\ 0&0&1&0&0&0\\ 0&0&0&0&0&0\\ \hline 0&0&0&0&0&0 \end{array}\right),\ T^{14} = \frac{1}{2}\left(\begin{array}{cc|ccc|c} 0&0&0&0&0&0\\ 0&0&0&0&0&0\\ \hline 0&0&0&-i&0&0\\ 0&0&i&0&0&0\\ 0&0&0&0&0&0\\ \hline 0&0&0&0&0&0 \end{array}\right),
$$

$$
T^{15} = \frac{1}{\sqrt{3}}\left(\begin{array}{cc|ccc|c} 0&0&0&0&0&0\\ 0&0&0&0&0&0\\ \hline 0&0&1&0&0&0\\ 0&0&0&1&0&0\\ 0&0&0&0&-2&0\\ \hline 0&0&0&0&0&0 \end{array}\right),
$$

(A.4)

$$T^{16} = \frac{1}{2}\left(\begin{array}{cc|ccc|c} 0&0&0&0&1&0\\ 0&0&0&0&0&0\\ \hline 0&0&0&0&0&0\\ 0&0&0&0&0&0\\ 1&0&0&0&0&0\\ \hline 0&0&0&0&0&0 \end{array}\right), T^{17} = \frac{1}{2}\left(\begin{array}{cc|ccc|c} 0&0&0&0&-i&0\\ 0&0&0&0&0&0\\ \hline 0&0&0&0&0&0\\ 0&0&0&0&0&0\\ i&0&0&0&0&0\\ \hline 0&0&0&0&0&0 \end{array}\right),$$

$$T^{18} = \frac{1}{2}\left(\begin{array}{cc|ccc|c} 0&0&0&0&0&0\\ 0&0&0&0&1&0\\ \hline 0&0&0&0&0&0\\ 0&0&0&0&0&0\\ 0&1&0&0&0&0\\ \hline 0&0&0&0&0&0 \end{array}\right), T^{19} = \frac{1}{2}\left(\begin{array}{cc|ccc|c} 0&0&0&0&0&0\\ 0&0&0&0&-i&0\\ \hline 0&0&0&0&0&0\\ 0&0&0&0&0&0\\ 0&i&0&0&0&0\\ \hline 0&0&0&0&0&0 \end{array}\right),$$

$$T^{20} = \frac{1}{2}\left(\begin{array}{cc|ccc|c} 0&0&0&0&0&0\\ 0&0&0&0&0&0\\ \hline 0&0&0&0&1&0\\ 0&0&0&0&0&0\\ 0&0&1&0&0&0\\ \hline 0&0&0&0&0&0 \end{array}\right), T^{21} = \frac{1}{2}\left(\begin{array}{cc|ccc|c} 0&0&0&0&0&0\\ 0&0&0&0&0&0\\ \hline 0&0&0&0&-i&0\\ 0&0&0&0&0&0\\ 0&0&i&0&0&0\\ \hline 0&0&0&0&0&0 \end{array}\right), \tag{A.5}$$

$$T^{22} = \frac{1}{2}\left(\begin{array}{cc|ccc|c} 0&0&0&0&0&0\\ 0&0&0&0&0&0\\ \hline 0&0&0&0&0&0\\ 0&0&0&0&1&0\\ 0&0&0&1&0&0\\ \hline 0&0&0&0&0&0 \end{array}\right), T^{23} = \frac{1}{2}\left(\begin{array}{cc|ccc|c} 0&0&0&0&0&0\\ 0&0&0&0&0&0\\ \hline 0&0&0&0&0&0\\ 0&0&0&0&-i&0\\ 0&0&0&i&0&0\\ \hline 0&0&0&0&0&0 \end{array}\right),$$

$$T^{24} = \frac{1}{\sqrt{15}}\left(\begin{array}{cc|ccc|c} 3&0&0&0&0&0\\ 0&3&0&0&0&0\\ \hline 0&0&-2&0&0&0\\ 0&0&0&-2&0&0\\ 0&0&0&0&-2&0\\ \hline 0&0&0&0&0&0 \end{array}\right),$$

$$
T^{25} = \frac{1}{2}\left(\begin{array}{cc|ccc|c} 0&0&0&0&0&1\\ 0&0&0&0&0&0\\ \hline 0&0&0&0&0&0\\ 0&0&0&0&0&0\\ 0&0&0&0&0&0\\ \hline 1&0&0&0&0&0 \end{array}\right),\ T^{26} = \frac{1}{2}\left(\begin{array}{cc|ccc|c} 0&0&0&0&0&-i\\ 0&0&0&0&0&0\\ \hline 0&0&0&0&0&0\\ 0&0&0&0&0&0\\ 0&0&0&0&0&0\\ \hline i&0&0&0&0&0 \end{array}\right),
$$

$$
T^{27} = \frac{1}{2}\left(\begin{array}{cc|ccc|c} 0&0&0&0&0&0\\ 0&0&0&0&0&1\\ \hline 0&0&0&0&0&0\\ 0&0&0&0&0&0\\ 0&0&0&0&0&0\\ \hline 0&1&0&0&0&0 \end{array}\right),\ T^{28} = \frac{1}{2}\left(\begin{array}{cc|ccc|c} 0&0&0&0&0&0\\ 0&0&0&0&0&-i\\ \hline 0&0&0&0&0&0\\ 0&0&0&0&0&0\\ 0&0&0&0&0&0\\ \hline 0&i&0&0&0&0 \end{array}\right),
$$

$$
T^{29} = \frac{1}{2}\left(\begin{array}{cc|ccc|c} 0&0&0&0&0&0\\ 0&0&0&0&0&0\\ \hline 0&0&0&0&0&1\\ 0&0&0&0&0&0\\ 0&0&0&0&0&0\\ \hline 0&0&1&0&0&0 \end{array}\right),\ T^{30} = \frac{1}{2}\left(\begin{array}{cc|ccc|c} 0&0&0&0&0&0\\ 0&0&0&0&0&0\\ \hline 0&0&0&0&0&-i\\ 0&0&0&0&0&0\\ 0&0&0&0&0&0\\ \hline 0&0&i&0&0&0 \end{array}\right),
$$

$$
T^{31} = \frac{1}{2}\left(\begin{array}{cc|ccc|c} 0&0&0&0&0&0\\ 0&0&0&0&0&0\\ \hline 0&0&0&0&0&0\\ 0&0&0&0&0&1\\ 0&0&0&0&0&0\\ \hline 0&0&0&1&0&0 \end{array}\right),\ T^{32} = \frac{1}{2}\left(\begin{array}{cc|ccc|c} 0&0&0&0&0&0\\ 0&0&0&0&0&0\\ \hline 0&0&0&0&0&0\\ 0&0&0&0&0&-i\\ 0&0&0&0&0&0\\ \hline 0&0&0&i&0&0 \end{array}\right),
$$

$$
T^{33} = \frac{1}{2}\left(\begin{array}{cc|ccc|c} 0&0&0&0&0&0\\ 0&0&0&0&0&0\\ \hline 0&0&0&0&0&0\\ 0&0&0&0&0&0\\ 0&0&0&0&0&1\\ \hline 0&0&0&0&1&0 \end{array}\right),\ T^{34} = \frac{1}{2}\left(\begin{array}{cc|ccc|c} 0&0&0&0&0&0\\ 0&0&0&0&0&0\\ \hline 0&0&0&0&0&0\\ 0&0&0&0&0&0\\ 0&0&0&0&0&-i\\ \hline 0&0&0&0&i&0 \end{array}\right),
$$

$$
T^{35} = \frac{1}{\sqrt{15}}\left(\begin{array}{cc|ccc|c} 1&0&0&0&0&0\\ 0&1&0&0&0&0\\ \hline 0&0&1&0&0&0\\ 0&0&0&1&0&0\\ 0&0&0&0&1&0\\ \hline 0&0&0&0&0&-5 \end{array}\right).
$$

(A.6)

B Wilson line in gGHU

In appendix B, we discuses the remaining symmetry of Gauge-Higgs unification. The gauge transformation of the gauge fields is

$$\mathcal{A}_M(x,y) \to \mathcal{A}'_M(x,y) = \Omega(x,y)\mathcal{A}_M(x,y)\Omega(x,y)^{-1} + \frac{i}{g}\Omega(x,y)\partial_M\Omega(x,y)^{-1}, \tag{B.1}$$

where $\Omega(x,y) = \exp(i\sum_a \alpha_a(x,y)T^a)$. Noting the periodic boundary condition of the gauge field $\mathcal{A}_M$ in Eq. (2.5), $2\pi R$ transformation of $\mathcal{A}'_M$ is obtained by

$$\begin{aligned}
\mathcal{A}'_M(x,y+2\pi R) &= \Omega(x,y+2\pi R)\mathcal{A}_M(x,y)\Omega(x,2\pi R)^{-1} \\
&\quad + \frac{i}{g}\Omega(x,2\pi R)\partial_M\Omega(x,2\pi R)^{-1} \\
&= \Omega(x,y+2\pi R)T^\dagger\mathcal{A}_M(x,y+2\pi R)T\Omega(x,2\pi R)^{-1} \\
&\quad + \frac{i}{g}\Omega(x,2\pi R)T^\dagger\partial_M T\Omega(x,2\pi R)^{-1} \\
&= T'\mathcal{A}'_M(x,y)T'^{-1},
\end{aligned} \tag{B.2}$$

where $T' = \Omega(x,y+2\pi R)T\Omega(x,y)^{-1}$. The remaining symmetries are obtained by invariance of the boundary condition,

$$T = \Omega(x,y+2\pi R)T\Omega(x,y)^{-1}. \tag{B.3}$$

The Wilson line is defined by

$$W(x) = \mathcal{P}\exp\left\{ig_5\int_0^{2\pi R} dy A_M(x,y)\right\}, \tag{B.4}$$

which transforms under the gauge transformation as

$$W(x) \to \Omega(x,0)W(x)\Omega(x,2\pi R)^{-1}. \tag{B.5}$$

The gauge transformation of the product of W and T under transformation satisfied the relation Eq. (B.3) is

$$\hat{W} = WT \to \Omega(x,0)W(x)\Omega(x,2\pi R)^{-1}T = \Omega(x,0)\hat{W}(x)\Omega(x,0)^{-1}. \tag{B.6}$$

Therefore the trace of product is gauge invariant under the remaining symmetries.

References

[1] N. Maru and Y. Yatagai, PTEP **2019**, no. 8, 083B03 (2019); arXiv:1903.08359 [hep-ph].

[2] N. Maru and Y. Yatagai, Eur. Phys. J. C, **80**(10):933 (2020); arXiv:1911.03465 [hep-ph].

[3] H. Takahashi, N. Maru and Y. Yatagai, arXiv:2205.05824 [hep-ph].

[4] H. Takahashi, N. Maru and Y. Yatagai, Phys. Rev. D **106**, 055033 (2022); arXiv:2207.10253 [hep-ph].

[5] N.S. Manton, Nucl. Phys. B **158**, 141 (1979); D.B. Fairlie, Phys. Lett. B **82**, 97 (1979), J. Phys. G **5**, L55 (1979); Y. Hosotani, Phys. Lett. B **126**, 309 (1983), Phys. Lett. B **129**, 193 (1983), Annals Phys. **190**, 233 (1989).

[6] H. Hatanaka, T. Inami and C.S. Lim, Mod. Phys. Lett. A **13**, 2601 (1998); I. Antoniadis, K. Benakli and M. Quiros, New J. Phys. **3**, 20 (2001); G. von Gersdorff, N. Irges and M. Quiros, Nucl. Phys. B **635**, 127 (2002); R. Contino, Y. Nomura and A. Pomarol, Nucl. Phys. B **671**, 148 (2003); C.S. Lim, N. Maru and K. Hasegawa, J. Phys. Soc. Jap. **77**, 074101 (2008).

[7] N. Maru and T. Yamashita, Nucl. Phys. B **754**, 127 (2006); Y. Hosotani, N. Maru, K. Takenaga and T. Yamashita, Prog. Thoer. Phys. **118**, 1053 (2007).

[8] C.S. Lim and N. Maru, Phys. Lett. B **653**, 320 (2007).

[9] G. Burdman and Y. Nomura, Nucl. Phys. B **656**, 3 (2003); N. Haba, Y. Hosotani, Y. Kawamura and T. Yamashita, Phys. Rev. D **70**, 015010 (2004); K. Kojima, K. Takenaga and T. Yamashita, Phys. Rev. D **84**, 051701 (2011); Phys. Rev. D **95**, no. 1, 015021 (2017); JHEP **1706**, 018 (2017); Y. Hosotani and N. Yamatsu, PTEP **2015**, 111B01 (2015); A. Furui, Y. Hosotani and N. Yamatsu, PTEP **2016**, no. 9, 093B01 (2016); Y. Hosotani and N. Yamatsu, PTEP **2017**, no. 9, 091B01 (2017); PTEP **2018**, no. 2, 023B05 (2018); S. Funatsu, H. Hatanaka, Y. Hosotani, Y. Orikawa and N. Yamatsu, Phys. Rev. D **99**, no. 9, 095010 (2019), Phys. Rev. D **102**, no.1, 015005 (2020); A. Angelescu, A. Bally, S. Blasi and F. Goertz, Phys. Rev. D **105**, no.3, 035026 (2022).

[10] C.A. Scrucca, M. Serone and L. Silvestrini, Nucl. Phys. B **669**, 128 (2003).

[11] C. Csaki, C. Grojean and H. Murayama, Phys. Rev. D **67**, 085012 (2003).

[12] K.R. Dienes, E. Dudas and T. Gherghetta, Phys. Lett. B **436**, 55 (1998); Nucl. Phys. B **537**, 47 (1999).

[13] Y. Kawamura, Prog. Theor. Phys. **105**, 999 (2001).

[14] P.A. Zyla *et al.* (Particle Data Group), Prog. Theor. Exp. Phys. **2020**, 083C01 (2020).

[15] T. Appelquist, B.A. Dobrescu, E. Ponton and H.U. Yee, Phys. Rev. Lett. **87**, 181802 (2001).